# Trade Policy and the Emissions Content of Agricultural Trade


**Abstract**

We study how trade policy shapes greenhouse gas emissions embodied in agricultural trade, linking structural gravity simulations to country–commodity farm-gate $CH_4$ and $N_2O$ emissions. Our results show that existing tariff preferences raise embodied emissions by 37.9 megatonnes of $CO_2$-equivalent, valued at about $3.4 billion annually using a recent carbon-border price, with livestock, especially beef, driving most of the increase. A zero-tariff benchmark, which reveals possible reallocations from continuing trade liberalization, is estimated to raise global $CH_4$ and $N_2O$ emissions by 17.7 megatonnes $CO_2$-equivalent, driven mainly by trade in crops, especially rice. Our findings illuminate how the existing global regime of tariff barriers shapes the environmental consequences of trade.



**JEL Codes**: F14; Q17; Q56
**Keywords**: Tariffs; Agricultural Trade; Embodied Emission; Greenhouse Gas; Structural Gravity

# 1 Introduction

Trade policy is a fundamental determinant of trade, production, and consumption. This fact implies that trade barriers such as tariffs play a key role in shaping the global patterns of pollution, including the emission of greenhouse gases (GHGs). This mechanism is especially important in agriculture, where trade barriers remain substantial and production is a major source of methane ($CH_4$) and nitrous oxide ($N_2O$). This paper asks how tariff policy influences the geography of agricultural production and trade, and through that channel, the farm-gate GHG emissions embodied in traded commodities.

Agricultural markets offer a particularly useful context in which to study this mechanism. The agricultural sector is a major source of $CH_4$ and $N_2O$, two GHGs with global warming potentials (GWPs) far exceeding that of carbon dioxide ($CO_2$). Agriculture was responsible for 69% and 41% of global emissions of these respective gases during the 2010–2019 period, and agricultural sources together accounted for around 10% of the world's total GHG emissions (Nabuurs et al., 2022).[1] While $CH_4$ and $N_2O$ exist in the atmosphere in smaller quantities than $CO_2$, their marginal warming effects are substantially larger.[2] At the same time, agricultural trade has expanded rapidly. Statistics from FAO (2024a) indicate that the real value of global agricultural production grew by 129.5% between 2002 and 2022, from \$1.9 trillion to \$4.3 trillion in 2015 dollars, while the real value of global crop exports increased by 180.2%, from \$560.0 billion to \$1.6 trillion. These trends make the agricultural sector an important setting for studying how trade policy influences the distribution of emissions across countries and products.[3]

Existing work has sought to quantify the emissions embodied in traded commodities, often through accounting exercises that trace emissions through observed trade flows (Johnson et al., 2007; Garnett, 2011; Hong et al., 2021, 2022). Less is known about the role of trade policy in mediating these patterns. This is an important gap because tariff barriers remain a central feature of the global trading system and because recent trade agreements increasingly incorporate environmental and sustainability provisions.[4] We address this gap by quantifying how tariff

[1] Agriculture is also a significant source of $CO_2$, accounting for 14% of global $CO_2$ emissions as of 2022 (Nabuurs et al., 2022).

[2] As of 2024, the atmospheric content of $CO_2$ measured around 402 parts per million (NOAA Climate Monitoring Lab; `https://gml.noaa.gov/ccgg/data`). This compares to atmospheric concentrations of $CH_4$ and $N_2O$ of around 1,935 and 338 parts per billion, respectively. Estimates of GWP place the marginal impacts of $CH_4$ and $N_2O$ at 28 and 265 times that of $CO_2$, respectively (Pachauri et al., 2014).

[3] International trade is also expected to play an important role as a channel for adaptation to climate change, as countries experiencing adverse climate impacts on agricultural production can mitigate domestic shortfalls through imports (Gouel and Laborde, 2021). Rising trade volumes associated with climate adaptation may further increase the environmental importance of agricultural trade.

[4] Several recently formed trade agreements include provisions that target environmental and sustainability objectives. In July 2024, negotiations between Costa Rica, Iceland, New Zealand and Switzerland were concluded on the Agreement on Climate Change, Trade and Sustainability (ACCTS), which contains provisions related to climate change, biodiversity loss, pollution, and other environmental concerns. Similarly, the European Union's Economic Partnership Agreement with Kenya, also established in 2024, contains a dedicated chapter on trade and sustainable development.

regimes shape the international distribution of farm-gate $CH_4$ and $N_2O$ emissions embodied in agricultural trade for seven major agri-food commodities, including beef, chicken, pork, maize, rice, soybeans, and wheat.[5]

We investigate these relationships using a structural gravity modeling approach, a workhorse methodology in empirical trade analysis. To do this, we map existing and potential tariff regimes into counterfactual trade flows and then combine those flows with information on observed country–commodity emission intensities. The resulting exercise measures the emissions content of trade implied by alternative trade policy scenarios: in particular, we examine how applied tariffs, preferential margins (the difference between preferential tariff rates and baseline non-discriminatory tariff rates), and remaining trade barriers shape the geography of agricultural trade, production, and consumption across countries with different farm-gate emission intensities.

Our empirical strategy proceeds in two steps. We first estimate a commodity-level gravity model using a panel of international and intranational trade flows (the latter reflecting the volume of trade within the domestic market), applicable bilateral tariff rates, and standard gravity covariates. The specification includes theory-consistent exporter–commodity–year and importer–commodity–year fixed effects, allowing us to recover commodity-specific estimates of trade elasticities while controlling for multilateral resistance and other time-varying origin- and destination-specific factors. We then use these estimates in counterfactual simulations based on the estimation-with-calibration procedure of Anderson et al. (2018). We translate simulated trade flows into embodied emissions using country- and commodity-specific farm-gate emission intensities for $CH_4$ and $N_2O$ under two distinct counterfactual scenarios.[6]

The first counterfactual replaces existing preferential tariffs with the corresponding non-discriminatory Most Favored Nation (MFN) tariff rates.[7] This experiment seeks to quantify the degree to which the preferential liberalization embedded in existing applied tariff schedules has influenced trade flows and the GHG emissions embodied in those flows. The second counterfactual sets all bilateral tariffs to zero to consider hypothetical global free trade. We treat

[5] We focus on these seven commodities because together they account for a substantial share of global agricultural trade and the overwhelming share of farm-gate GHG emissions from agriculture. Among livestock, cattle, pigs, and poultry are major contributors to agricultural GHG emissions, accounting for approximately 62%, 14%, and 9% of global emissions from livestock, respectively, according to the Food and Agriculture Organization of the United Nations (FAO, 2023). Among crop products, rice is particularly important, accounting for roughly 12% of global agricultural GHG emissions, primarily through $CH_4$ emissions generated from anaerobic paddy cultivation (Xu et al., 2021).

[6] Our analysis focuses on farm-gate emissions embodied in traded agricultural products. It does not include downstream processing, transportation, land-use change, or other emissions outside the farm gate. Trade also generates indirect emissions from transportation; estimates suggest that this channel accounts for about 19% of global food-system emissions (Li et al., 2022).

[7] MFN is the non-discriminatory principle of treating trade partners to which MFN status has been granted "no worse" than other partners receiving MFN treatment. MFN treatment is automatically conferred between all members of the World Trade Organization (WTO), which includes nearly all of the world's major economies. In the context of tariffs, MFN duties differ from preferential duties, such as those negotiated under preferential trade agreements, in that preferential duties are trade-pair-specific and are lower than the corresponding MFN rate.

this scenario not as a likely near-term policy forecast, but as an opposing benchmark to the MFN experiment; namely, this scenario measures the extent to which trade and emissions reallocations are constrained by the tariff barriers existing under the current global trade policy regime. Together, the two experiments allow us to evaluate the current system of global tariffs from two perspectives: the first measuring how existing tariff reductions have influenced the patterns of trade-embodied emissions, and the second exploring the potential impacts of hypothetical further tariff reductions.

Our main findings are as follows. First, tariff preferences are estimated to have increased global trade-embodied farm-gate emissions by 31.7 kilotonnes (kt) of $N_2O$ and 1,053.9 kt of $CH_4$ in 2022, equivalent to 37.9 megatonnes (Mt) of $CO_2$-equivalent ($CO_2e$) emissions.[8] Valued at the first official EU Carbon Border Adjustment Mechanism (CBAM) certificate price, this increase corresponds to an implied annual carbon value of approximately $3.4 billion.[9] The effect is highly concentrated across products and regions: livestock products, especially beef, account for most of the increase, with large changes involving France, the United States, and other countries with large livestock sectors and/or highly emissions-intensive livestock production, while rice drives much of the crop-related response, especially through major rice-producing or -consuming countries such as China, South Korea, and Thailand.

Second, hypothetical complete trade liberalization is estimated to increase trade-embodied emissions by approximately 17.7 Mt of $CO_2e$, but through different margins than under the first counterfactual. Removing all remaining tariffs does not simply intensify the patterns observed under the MFN counterfactual. Instead, it changes which countries, products, and trade relationships drive the emissions response. The United States becomes less prominent under full liberalization as reallocations across partner markets partly offset one another. South Korea and Japan—both of which maintain extensive barriers to agricultural imports—become much more prominent in the global distribution of trade-embodied GHG emissions once remaining tariff barriers are removed. China too remains a central country in trade-embodied GHGs, especially in rice trade. The zero-tariff scenario also magnifies the role of major agricultural exporters or importers such as Brazil, Iran, and Turkey, countries which are comparatively less central in the preference-removal experiment. The environmental consequences of trade policy therefore hinge on the specific countries, products, and tariff regimes under consideration.

Our study contributes to three areas of the literature. First, we build on work at the agriculture-environment intersection, especially studies of agricultural GHG emissions.[10] Related work in-

[8] $CO_2e$ emissions are calculated using GWPs for $N_2O$ and $CH_4$ relative to $CO_2$.

[9] The European Commission reports that quarterly CBAM certificate prices are calculated from publicly available information on EU Emissions Trading System auctions and apply to emissions embodied in CBAM goods imported into the European Union during the relevant quarter. Fastmarkets reports the first-quarter 2026 CBAM certificate price as €75.36, or $89.64, per tonne of $CO_2e$. Multiplying 37.9 Mt of $CO_2e$ by $89.64 per tonne of $CO_2e$ gives approximately $3.4 billion.

[10] See Vermeulen et al. (2012) for a survey of the literature on agriculture and GHG emissions. Lichtenberg (2002)

cludes Johnson et al. (2007) and Garnett (2011), who identify key sources of GHG emissions in the global agri-food system, and Hong et al. (2021, 2022), who quantify the embodied GHG content of traded agricultural products. We extend this literature by focusing on trade policy as a driver of embodied agricultural emissions.[11] Closely related is Verburg et al. (2009), who measure the contribution of agricultural trade liberalization to land-use-related GHG emissions for beef, milk, and dairy using a computable general equilibrium modeling approach. We build on this work by using a theory-consistent structural gravity framework that allows us to directly estimate the key parameters governing the responsiveness of trade flows to tariff barriers while considering a substantially larger set of countries and commodities.

Second, we contribute to the broader trade–environment literature. Within this area, Shapiro (2016) analyzes the role of trade costs in determining global $CO_2$ emissions, while Shapiro (2021) shows how tariff barriers affect $CO_2$ emissions by influencing imports of clean versus dirty inputs. Liu et al. (2020) examines how retaliatory trade barriers imposed under the U.S.–China trade war influenced countries' GHG emissions. Related work by Park et al. (2024) examine how changes in bilateral trade costs influence the distribution of emissions within and across countries. Other studies have measured embodied emission or natural resource content of trade using accounting-based approaches, such as environmentally extended multi-regional input-output models (e.g., Bruckner et al., 2012; Xu and Dietzenbacher, 2014; Aichele and Felbermayr, 2015; Chen et al., 2018). Closest in methodology to our analysis is Park and Ridley (2025), who employ structural gravity counterfactuals to study virtual water embodied in agricultural trade. Our analysis differs in both objectives and policy relevance. We study GHG emissions, a global externality with direct climate damages, and focus on $CH_4$ and $N_2O$, two gases for which the agricultural sector is a major source. This distinction matters because the relevance of examining how trade influences the use of water and other natural resources is, in general, location-specific, whereas reallocating GHG emissions affects a global stock externality. This paper therefore uses a similar empirical approach to address a different trade–environment question: namely, how import tariffs influence the emissions content of agricultural trade, and therefore, the implications of trade policy for climate change.

Third, our analysis contributes to the literature on trade policy in agricultural markets, particularly work using structural gravity models to quantify the impacts of tariffs, trade agreements, and other policies. Recent examples include Luckstead (2022), Ridley and Devadoss (2023), Larch et al. (2024), Dadakas et al. (2025), and Ridley and Shirin (2025). We extend this literature by linking the standard trade-policy counterfactuals generated by structural gravity models to country–commodity-specific emission intensities. This allows us to quantify not only how tariff regimes

provides an overview of earlier research on agriculture and environmental outcomes.

[11] By contrast, a growing literature examines how GHG emissions and climate change affect (or will affect) global agricultural production and trade. Recent examples include Costinot et al. (2016), Nath (2025), and Hultgren et al. (2025).

influence agricultural trade flows, but also where the associated farm-gate GHG emissions are reallocated under counterfactual changes in bilateral trade barriers.

The remainder of the paper is organized as follows. Section 2 provides background on agricultural emissions and the trade policy environment in global agricultural markets. Section 3 describes the structural gravity framework, the counterfactual simulation procedure, and the data. Section 4 presents the estimation and simulation results. Section 5 concludes.

# 2 Background on Agricultural Emissions and Trade Policy

This section documents two empirical facts that motivate the analysis: (i) emissions differ sharply across agricultural commodities and countries; and (ii) tariff preferences vary substantially across the markets in which those commodities are traded.

## 2.1 Global Farm-Gate Emissions from Agriculture

Agricultural emissions are concentrated in a small number of commodities and production processes. Livestock production is the dominant source of agricultural $CH_4$, largely through enteric fermentation in ruminant animals,[12] while crop production accounts for a substantial share of $CH_4$ and nearly all agricultural $N_2O$ emissions. Crop-related emissions arise from anaerobic decomposition in rice paddies, microbial activity in crop residues, synthetic fertilizer application, and residue burning. This concentration matters because tariff-induced trade reallocations have different ramifications for global GHG emissions depending on which commodities are impacted and where these commodities are produced.

Table 1 documents the commodity-level heterogeneity that underlies the counterfactual analysis. Among livestock products, beef is by far the largest source of farm-gate $CH_4$ emissions, reflecting both its scale of production and its high emission intensity.[13] On average, beef generates 255.7 kt of $CH_4$ per year, with a corresponding emission intensity of 1.3 tonnes per tonne of output. Pork also contributes sizable emissions, while chicken is much less emission-intensive among the animal products considered.

Among crops, rice accounts for a major portion of global GHG emissions. Average global $CH_4$ emissions from rice amount to 186.3 kt annually, and its average $CH_4$ and $N_2O$ intensities are 49.9

[12] Enteric fermentation in the digestive systems of ruminant livestock is estimated to be responsible for around 60% of the total $CH_4$ generated by the global agri-food system (FAO, 2024b).

[13] In analyzing livestock products, we constrain our analysis to meat products rather than other animal-derived goods such as dairy or eggs. We do this for several reasons. First, livestock production for meat accounts for a significantly larger share (roughly 75%; FAO, 2024a) of global farm-gate GHG emissions than livestock production for other purposes. Second, trade in non-meat animal products such as dairy is dominated by processed products such as cheese for which direct farm-gate emissions account for a comparatively smaller share of products' embodied emissions content. Third and more practically, suitable data with which to map farm-gate emissions from primary livestock production to specific non-meat animal products—and in turn, the highly specific commodity nomenclatures under which such goods are recorded in international trade and tariff statistics—is generally not available.

**Table 1:** Emissions and Emission Intensities by Commodity

| Commodity | $CH_4$ emissions | $N_2O$ emissions | $CH_4$ intensity | $N_2O$ intensity |
|---|---|---|---|---|
| Beef | 255,706.6 | 7,674.6 | 1,320.3 | 48.0 |
| Rice | 186,251.5 | 1,289.8 | 49.9 | 15.1 |
| Pork | 21,328.7 | 1,101.2 | 111.1 | 13.3 |
| Maize | 2,757.1 | 920.5 | 7.6 | 0.6 |
| Wheat | 1,876.8 | 1,398.3 | 0.5 | 0.3 |
| Chicken | 1,173.1 | 775.1 | 7.0 | 4.5 |
| Soybeans | 0.0 | 637.9 | 0.0 | 0.3 |

*Notes:* Table reports the average emissions and emission intensities for seven commodities over the period 2000–2021. The units for emissions are tonnes, and emission intensities are measured in tonnes of emissions per kilotonne of output. Data are sourced from the Food and Agriculture Organization (FAO).

and 15.1 tonnes per kilotonne of output, respectively. Other crops, including maize, soybeans, and wheat, contribute less individually, especially for $N_2O$, but remain important for comprehensively accounting for embodied emissions in traded agricultural products.

To complement the information on commodity-level emissions, Figures 1 and 2 present the geographical distribution of emissions of $CH_4$ and $N_2O$ across countries for the top four commodity sources of farm-gate GHG emissions from agricultural production, which include cattle, maize, rice, and wheat. The figures illustrate notable spatial disparities in emissions of $CH_4$ versus $N_2O$, both across countries and across commodities. For $CH_4$, many large agricultural producers account for outsize volumes of emissions, including Argentina (for beef, maize, and rice), Australia (beef), Brazil (beef, maize, rice), China (beef, maize, rice, wheat), India (beef, or more specifically, water buffalo, and rice), and the United States (beef, maize, rice, and wheat), among others. Similar disparities are apparent in global emissions patterns for $N_2O$, such that a diverse, geographically dispersed set of countries generate large volumes of this GHG through their production of particular commodities.

### 2.2 Tariff Barriers in Global Agricultural Markets

Agricultural markets remain among the more protected segments of world trade. As of 2023, applied MFN tariff rates averaged 15.4% for agricultural products, compared with 4.6% for non-agricultural products, based on information from the WTO World Tariff Profiles. Protection is especially high in the product categories central to our analysis: average MFN tariffs were 13.6% for crop products and 19.2% for animal products. These tariff barriers matter because even modest changes in market access can reallocate trade across countries with different farm-gate emission intensities.

At the same time, agricultural trade has liberalized gradually over the past several decades. A central feature of this liberalization has been the shift away from non-discriminatory MFN tariffs

**Figure 1:** Farm-Gate Emissions of $CH_4$ by Country from Top Four Commodity Sources

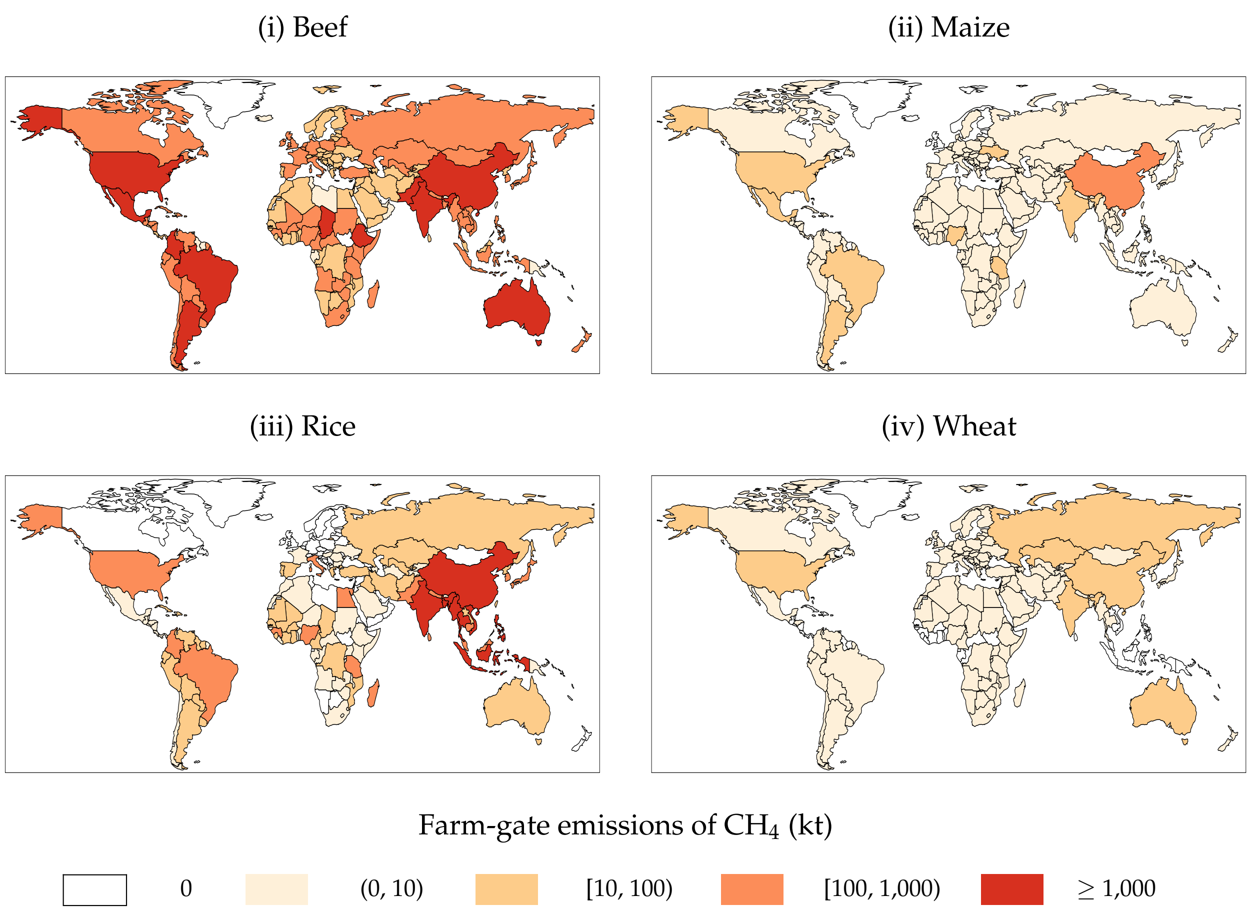


*Notes:* Authors' construction based on data for 2022 from FAO (2024a).

**Figure 2:** Farm-Gate Emissions of $N_2O$ by Country from Top Four Commodity Sources

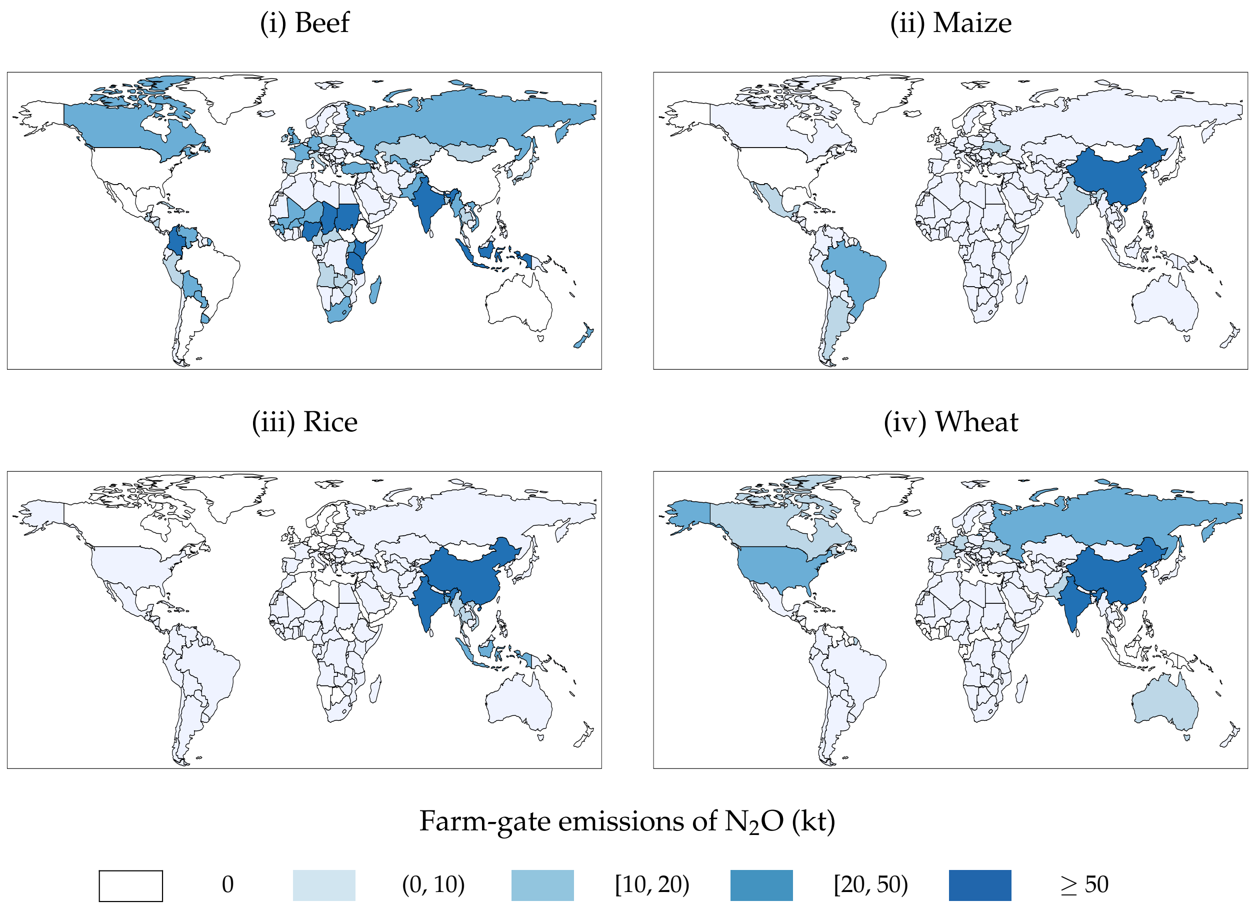


*Notes:* Authors' construction based on data for 2022 from FAO (2024a).

**Figure 3:** Value of Global Trade by Commodity under MFN versus Preferential Tariffs

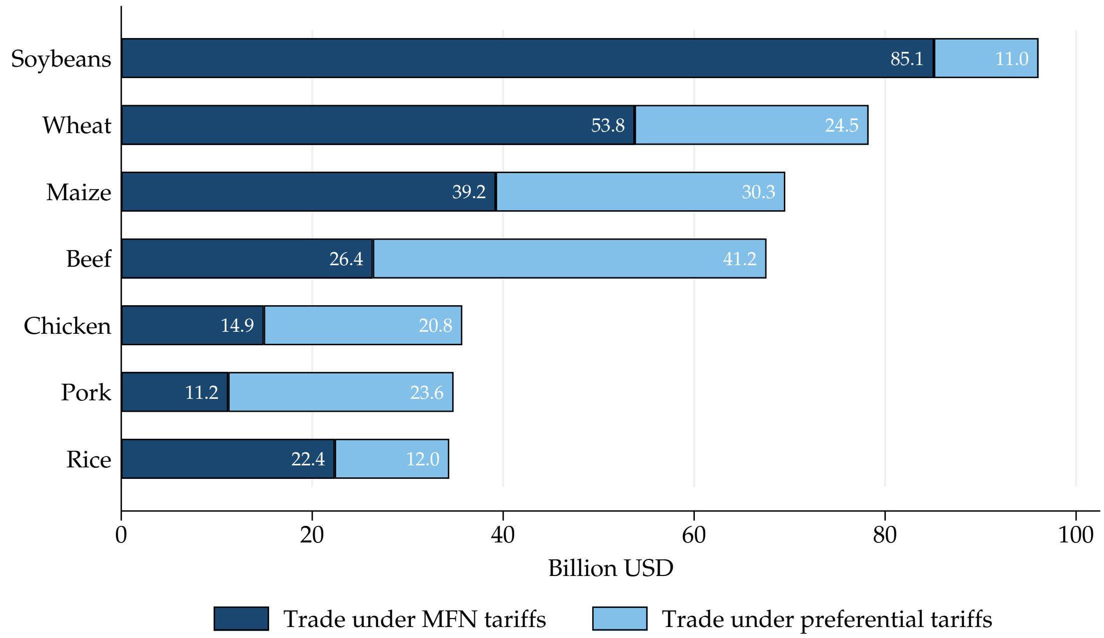


*Notes:* Figure displays total global trade in the indicated commodities for the year 2022 in billion current U.S. dollars, broken down by trade occurring under MFN versus preferential tariff rates. The labels on each bar indicate the value of global trade that occurs under the respective tariff category. Authors' construction based on data from CEPII (Gaulier and Zignago, 2010) and WITS (World Bank, 2025).

toward preferential tariff regimes. Tariff preferences are established through either reciprocal arrangements, such as regional trade agreements, and non-reciprocal programs, such as the Generalized System of Preferences in which advanced economies maintain low or zero tariffs on imports from lower income countries. As a result, the tariff actually applied to trade between a given country pair for a particular commodity often differs from the importer's non-discriminatory MFN rate.

Figure 3 illustrates this distinction for the commodities in our analysis by reporting the value of global trade conducted under MFN versus preferential tariffs. The figure highlights substantial heterogeneity across products. Some commodities, such as beef and pork, are traded largely under preferential rates, while others, such as soybeans, wheat, and rice, are more frequently traded under MFN tariffs. This heterogeneity motivates our two counterfactual experiments. Replacing preferential tariffs with MFN rates isolates the trade and emissions effects of preferential liberalization already embedded in current tariff schedules, while setting all tariffs to zero captures the additional reallocations that would occur if the remaining tariff barriers were removed.

Taken together, the stylized facts presented above characterize the global distribution of farm-gate GHG emissions from agriculture and the system of tariff barriers that influence international agricultural trade. To quantify how the latter mediates the former, particularly through the emissions content embodied in traded agricultural commodities, we implement a counterfactual-simulation-based empirical analysis to assess the link between the two.

# 3 Methodology

The preceding section shows that agricultural commodities differ sharply in their farm-gate emission intensities and in the tariff regimes under which they are traded. We now describe how we use this variation to quantify the emissions consequences of trade policy. The analysis proceeds in two steps. We first estimate a commodity-level structural gravity model to recover estimates on the parameters that govern the responsiveness of trade flows to tariffs. We then implement the simulation procedure of Anderson et al. (2018) to evaluate how alternative tariff regimes determine trade flows and the emissions embodied in those flows.

## 3.1 Econometric Methodology

Our empirical approach is based on the generalized version of the gravity equation (Anderson and van Wincoop, 2004; Fally, 2015) given by

$$X_{ijkt} = \frac{Y_{ikt}}{\Pi_{ikt}^{-\theta_k}} \frac{E_{jkt}}{P_{jkt}^{-\theta_k}} \tau_{ijkt}^{-\theta_k}. \tag{1}$$

$X_{ijkt}$ is the monetary value of exports from source region $i$ to destination region $j$ of commodity $k$ in year $t$, which includes both international ($i \neq j$) and intranational ($i = j$) flows.[14] Trade flows are a function of three main factors, the first of which are the market size terms describing total supply in region $i$, $Y_{ikt}$ (the value of region $i$'s total production of commodity $k$, with $Y_{ikt} = \sum_j X_{ijkt}$), and total demand in region $j$, $E_{jkt}$ (the value of region $j$'s total expenditures on commodity $k$). Intuitively, these terms reflect the logic that trade partners with larger supply and/or larger demand will engage in higher levels of trade, all else equal.

The remaining elements of Equation (1) are the trade cost terms, which consist of both bilateral ($\tau_{ijkt}$) and multilateral components ($\Pi_{ikt}$ and $P_{jkt}$). The term $\tau_{ijkt}$ captures all bilateral factors (time-varying and time-invariant) that encourage or impede trade, such as policy-related, geographical, or cultural factors. Bilateral trade costs enter multiplicatively according to the commonly used "iceberg" form, which is equivalent to assuming that a portion of the value of traded goods is lost in transit. $\Pi_{ikt}$ and $P_{jkt}$ are the outward and inward multilateral resistance terms (MRTs), first

[14] Yotov (2022) describes an assortment of important benefits provided by the inclusion of intranational trade flows in gravity estimations: among others, consistency with theory and sharper estimates of trade policy parameters. Intranational trade flows are also a necessary element of our simulation analysis, in that their inclusion allows us to assess how trade policy causes trade flows to be reallocated between domestic and international markets.

formalized by Anderson and van Wincoop (2003), and are defined as

$$\Pi_{ikt}^{-\theta_k} = \sum_{j=1}^{N} \frac{E_{jkt}\tau_{ijkt}^{-\theta_k}}{P_{jkt}^{-\theta_k}} \quad \text{and} \quad P_{jkt}^{-\theta_k} = \sum_{i=1}^{N} \frac{Y_{ikt}\tau_{ijkt}^{-\theta_k}}{\Pi_{ikt}^{-\theta_k}}. \tag{2}$$

The MRTs correspond to consumption- and production-weighted average incidences of trade costs faced by exporter $i$ and importer $j$, respectively. Importantly, these terms' definitions imply that changes in bilateral trade costs between any pair of trading partners $i$ and $j$ will impact trade between any other pair $i'$ and $j'$ due to resulting adjustments in the MRTs. Finally, $\theta_k > 0$ is the trade elasticity, which measures the sensitivity of bilateral trade flows to changes in trade costs. Estimates of $\theta_k$ will serve as a key parameter input in our counterfactual simulation analysis.

We parameterize bilateral trade costs as a function of tariffs and standard non-tariff determinants of trade costs given by

$$\tau_{ijkt}^{-\theta_k} = \exp\left\{-\theta_k \log\left(1 + t_{ijkt}\right) + \boldsymbol{Z}_{ij}\boldsymbol{\beta}_k\right\}. \tag{3}$$

The term $\log\left(1 + t_{ijkt}\right)$ is the natural logarithm of the applicable bilateral tariff rates ($t_{ijkt}$) in gross ad valorem terms.[15] To account for non-ad valorem tariffs (specific tariffs, compound tariffs, or tariff-rate quotas), we use calculations of ad valorem equivalents (AVEs) that re-express non-ad valorem tariffs in percentage terms (we describe this aspect of our data in more detail below). To account for observable bilateral trade costs between trading partners, we define $\boldsymbol{Z}_{ij}$ with associated parameter vector $\boldsymbol{\beta}_k$ as a set of bilateral geographical and cultural factors commonly used in the gravity literature to capture long-run determinants of trade costs:

$$\boldsymbol{Z}_{ij}\boldsymbol{\beta}_k = \beta_{1k}\log(\text{DIST}_{ij}) + \beta_{2k}\text{CNTG}_{ij} + \beta_{3k}\text{COMLANG}_{ij}. \tag{4}$$

$\log(\text{DIST}_{ij})$ represents the natural logarithm of the bilateral distance between countries $i$ and $j$. The remaining terms $\text{CNTG}_{ij}$ and $\text{COMLANG}_{ij}$ are binary indicators that equal one for trading partners sharing a contiguous border or common official language, respectively, and zero otherwise. $\boldsymbol{\beta}_k$ thus measures the effect of observable bilateral trade cost variables (conditional on the effects of preferential tariffs) on bilateral trade.

Substituting Equation (3) into Equation (1), manipulating, and including a stochastic error term yields our regression specification given by

$$X_{ijkt} = \exp\left\{-\theta_k \log(1 + t_{ijkt}) + \boldsymbol{Z}_{ij}\boldsymbol{\beta}_k + \gamma_{ikt} + \delta_{jkt}\right\} + \varepsilon_{ijkt}. \tag{5}$$

The fixed effects $\gamma_{ikt} = \log\left(Y_{ikt}\right) + \theta_k \log\left(\Pi_{ikt}\right)$ and $\delta_{jkt} = \log\left(E_{jkt}\right) + \theta_k \log\left(P_{jkt}\right)$ capture the market size terms ($Y_{ikt}$ and $E_{jkt}$) as well as the outward and inward MRTs ($\Pi_{ikt}$ and $P_{jkt}$). These

[15] See Fontagné et al. (2022) for a derivation of the functional relationship between bilateral trade flows and tariffs in the structural gravity setting.

fixed effects also account for all other time-varying exporter- and importer-specific factors, which include any unilateral determinants of trade such as non-discriminatory trade policies (thus controlling for most non-tariff measures affecting trade, which are typically non-discriminatory in nature), domestic policies, endowments, consumer preferences, technological progress, and other factors. By directly capturing the influence of the MRTs, these terms will also mediate the multilateral impacts of counterfactual changes in bilateral trade policy as we will explore in our simulation analysis. Finally, $\varepsilon_{ijkt}$ is a mean-zero error term, which we cluster at the country-pair level to flexibly accommodate within-pair correlations.

Following Santos Silva and Tenreyro (2006) and what has become standard in the literature, we estimate Equation (5) using Poisson pseudo-maximum likelihood (PPML). PPML has the advantages relative to log-linearized forms of gravity of accommodating zero-valued trade flows and being unbiased and consistent in the presence of heteroskedasticity.

## 3.2 Simulation Methodology

Based on the structural framework outlined above, our simulation approach evaluates how trade policy affects trade flows and the emissions embodied in them. To do so, we use the "estimation-with-calibration" procedure of Anderson et al. (2018), comparing trade outcomes under the observed tariff structure with those under a counterfactual regime. The baseline scenario reflects the commodity-specific bilateral tariff rates actually applied to trade within each country pair, whether preferential or MFN.

We consider two counterfactual scenarios. The first removes all preferential margins and reverts all tariffs to each country's non-discriminatory MFN schedule. The second assumes full trade liberalization, setting all global tariffs to zero. The comparisons yielded by these scenarios provide direct measures of the cumulative impact of preferential liberalization and the broader effects of full trade liberalization, thus revealing the extent to which current embodied GHG trade patterns are shaped by tariff barriers. In all scenarios, we fix the period of analysis to 2022, the latest year in our sample; consequently, we omit the time notation $t$ from the following description.[16]

The simulation procedure is implemented as follows. First, we obtain baseline trade flows by re-estimating a version of Equation (5) that imposes the estimated parameter values on all right-hand-side variables but the exporter–commodity and importer–commodity fixed effects $\gamma_{ik}$ and $\delta_{jk}$:

$$X_{ijk} = \exp\left\{-\widehat{\theta}_k \log(1 + t^{\mathrm{B}}_{ijk}) + \boldsymbol{Z}_{ij}\widehat{\boldsymbol{\beta}}_k + \gamma_{ik} + \delta_{jk}\right\} + \varepsilon_{ijk}, \tag{6}$$

where superscript B terms indicate values under the baseline scenario and hat notation indicates parameter estimates. Estimation of Equation (6) yields values for the exporter–commodity and

[16] 2022 is the latest year for which comprehensive information on emission intensities by country and commodity is available from FAO.

importer–commodity fixed effects $\gamma_{ik}$ and $\delta_{jk}$. Baseline bilateral trade flows are then computed using the predicted values from the regression of Equation (6):

$$X^{\mathrm{B}}_{ijk} = \exp\left\{-\widehat{\theta}_k \log(1+t^{\mathrm{B}}_{ijk}) + \boldsymbol{Z}_{ij}\widehat{\boldsymbol{\beta}}_k + \widehat{\gamma}^{\mathrm{B}}_{ik} + \widehat{\delta}^{\mathrm{B}}_{jk}\right\}. \tag{7}$$

In essence, the calculation in Equation (7) allows us to separately identify both the bilateral (direct) and multilateral (indirect) influences of trade costs on trade flows. The former are mediated by the term $-\widehat{\theta}_k \log(1+t^{\mathrm{B}}_{ijk})$. The latter are governed by the estimates $\widehat{\gamma}^{\mathrm{B}}_{ik}$ and $\widehat{\delta}^{\mathrm{B}}_{jk}$, which, as shown by Fally (2015), are proportional to the values of $\Pi_{ik}$ and $P_{jk}$ that would otherwise be obtained through numerical solution of Equation (2). Estimates of these fixed effects thus capture the multilateral effects of changes in tariffs between any pair of countries in the trading system.

Counterfactual trade flows are obtained in a similar fashion. The parameter values yielded from estimation of Equation (5) are used to re-estimate the equation

$$X_{ijk} = \exp\left\{-\widehat{\theta}_k \log(1+t^{\mathrm{C}}_{ijk}) + \boldsymbol{Z}_{ij}\widehat{\boldsymbol{\beta}}_k + \gamma_{ik} + \delta_{jk}\right\} + \varepsilon_{ijk}, \tag{8}$$

where superscript C denotes values under either of the two counterfactual scenarios. The predicted values from estimation of Equation (8) are then used to compute counterfactual bilateral trade values as

$$X^{\mathrm{C}}_{ijk} = \exp\left\{-\widehat{\theta}_k \log(1+t^{\mathrm{C}}_{ijk}) + \boldsymbol{Z}_{ij}\widehat{\boldsymbol{\beta}}_k + \widehat{\gamma}^{\mathrm{C}}_{ik} + \widehat{\delta}^{\mathrm{C}}_{jk}\right\}. \tag{9}$$

Analogous to Equation (7), the term $-\widehat{\theta}_k \log(1+t^{\mathrm{C}}_{ijk})$ measures the bilateral influence of tariffs on counterfactual trade flows. The estimates $\gamma^{\mathrm{C}}_{ik}$ and $\delta^{\mathrm{C}}_{jk}$ similarly account for the multilateral effects of assumed counterfactual trade costs on trade flows. In this setting, however, these terms are proportional to the values of the MRTs under the counterfactual trade policy regime.

Because trade flows $X_{ijk}$ reflect monetary values and our ultimate objective is to measure the volume of trade-embodied farm-gate emissions, the final step is to convert values into implied emissions content. This involves two steps. We first express traded values as traded quantities using information on the unit value of exports drawn from our underlying data:

$$Q_{ijk} = X_{ijk}/P_{ik}, \tag{10}$$

where $Q_{ijk}$ is the quantity of exports and $P_{ik}$ (the unit value of exports) is calculated using information on total export values and quantities by exporter and commodity.

We compute the emissions content embodied in each trading relationship ($E_{ijk}$) using information on emission intensity factors:

$$E_{ijk} = e_{ik} \times Q_{ijk}, \tag{11}$$

where $e_{ik}$ is the emissions per unit of output generated in exporter $i$'s production of commodity $k$.[17] We perform the calculation in Equation (11) separately for emissions of $CH_4$ and $N_2O$; however, to present the results for each pollutant in a comparable way, we convert the calculated emissions content of trade for each into a single $CO_2$e value using estimates of the GWP equal to 28 for $CH_4$ and 265 for $N_2O$ as described in the fifth report of the Intergovernmental Panel on Climate Change (IPCC; Pachauri et al., 2014).

Finally, for each counterfactual scenario, we compute the emissions difference as

$$\Delta E_{ijk} = E_{ijk}^{\mathrm{B}} - E_{ijk}^{\mathrm{C}}. \tag{12}$$

$E_{ijk}^{\mathrm{B}}$ denotes emissions under the observed applied tariff regime, and $E_{ijk}^{\mathrm{C}}$ denotes emissions under the relevant counterfactual. Thus, in the MFN exercise, positive values mean that existing tariff preferences have *increased* embodied emissions relative to the MFN benchmark. In the zero-tariff exercise, on the other hand, positive values mean that full liberalization would *reduce* embodied emissions relative to the current regime, whereas negative values mean that further liberalization would *increase* them.

### Data and Summary Statistics

The data that we use consists of three main pieces of information: (i) bilateral trade flows (both international and *intra*national); (ii) applicable bilateral tariff rates and gravity control variables; and (iii) country–commodity-level emission factors (i.e., volume of emissions per unit of production).[18] These data and their sources are described below.

**Inter- and Intranational Trade.** International trade flows in terms of both value and quantity are sourced from the *Base pour l'Analyse du Commerce International* (BACI) dataset on bilateral trade produced by the *Centre d'Etudes Prospectives et d'Informations Internationales* (CEPII; Gaulier and Zignago 2010). BACI records annual bilateral trade flows according to the 6-digit Harmonized System (HS) commodity nomenclature and reconciles differences in the declared customs value of trade as reported by the exporter and importer in each trading relationship.[19] Intranational trade flows are calculated manually using information from FAO databases on production, exports, and prices. We specifically calculate this information by first computing the difference between countries' quantities of production and exports, with this residual reflecting the volume of domestic sales (output sold in the domestic market). These quantities are then translated into

[17] While emission intensities can differ between producers and regions within a country (Barrozo, 2024; Park et al., 2024), comprehensive data that would allow us to account for this does not exist. We thus calculate emission intensities in terms of the *average* farm-gate emissions per unit of output by country and commodity.

[18] The full list of countries included in the analysis is given in Table A1.

[19] The 4-digit HS codes associated with the commodities in our analysis include 0201 and 0202 (beef), 0203 (pork), 0207 (poultry), 1001 (wheat), 1005 (maize), 1006 (rice), and 1201 (soybeans). These commodity codes map directly to the definitions used to define products in the FAO data.

monetary values using information on farm-gate prices for each country and commodity.[20]

**Tariffs and Gravity Variables.** Data on tariffs come from the Trade Analysis Information System (TRAINS) database, accessed through the World Bank's World Integrated Trade Solution (WITS) platform. Our tariff measure is the applicable bilateral tariff rate for each commodity and trading pair, calculated as averages at the HS 4-digit level to conform to our trade data.[21] When a preferential tariff is reported, the measure takes that preferential rate; when no preferential rate is reported, it takes the importer's MFN tariff for the corresponding commodity. For tariffs levied in non-ad-valorem form, such as specific, compound, or tariff-rate quota measures, we use the AVE values reported in WITS when available. Tariffs are set to zero for all observations of intranational trade.[22]

Information on the gravity control variables (bilateral distance, contiguous border, and common language) is obtained from the USITC's Dynamic Gravity Dataset version 2.1 (Gurevich and Herman, 2018). This dataset provides comprehensive information on these variables for effectively all country pairs. Bilateral distances, which include internal (within-country) distance, are calculated as population-weighted great-circle measures.

**Emission Intensities.** As described earlier, we obtain data on farm-gate emission intensities for $CH_4$ and $N_2O$ by country and commodity from FAO. Emission intensities are calculated by FAO as the ratio of GHG (in tonnes) emissions associated with each given commodity and production of that commodity (in kt) calculated based on reported national production data.

Table 2 provides summary statistics on the main variables used in the empirical analysis (besides emissions and emission intensities, information on which is reported above in Table 1).[23] The observations on trade flows show a combination of large intranational flows and smaller international flows, the former reflective of the typically much larger size of domestic markets relative to international trade linkages. The tariff data also reveal substantial variation across country pairs and commodities: the average applied rate is 17.5 percent, and the associated wide dispersion reflects the coexistence of MFN tariffs, preferential rates, and high-tariff observations in certain highly protectionist countries. The remaining variables reflect standard sources of bilateral trade

[20] This calculation involves several other adjustments to account for features of the underlying data. First, for a small number of countries, the difference between production and exports is calculated to be negative; this predominately occurs in cases of large transhipment destinations such as Hong Kong, Singapore, or the United Arab Emirates. Given that such economies typically do not produce any of the commodities under consideration or produce only negligible quantities, we record intranational trade as zero in such cases. A second issue relates to missing price information for some countries and commodities. In instances of countries with positive production of a commodity but for which no farm-gate prices are recorded by FAO, we interpolate the missing price information with production-share-weighted regional average prices.

[21] Applied bilateral tariffs for beef are calculated as the average across HS codes 0201 and 0202.

[22] As documented by Teti (2024) and others, the primary tariff data reported in WITS contain numerous missing observations, especially in the earlier years of the sample, generally prior to 2000. This issue arises because not all countries report tariffs in each year. For countries with incomplete tariff information, we interpolate missing observations using the most recently reported applicable tariff rate for each commodity.

[23] Summary statistics on trade flows and tariff rates for individual commodities are presented in Appendix Table A2.

**Table 2:** Descriptive Statistics

| Variables | Mean | Std. dev. | Min | Max |
|---|---|---|---|---|
| Intranational trade ($X_{ij}$ for $i = j$) | 319.3 | 2,984.5 | 0 | 170,611.4 |
| International trade ($X_{ij}$ for $i \neq j$) | 0.3 | 21.3 | 0 | 27,235.1 |
| Tariffs (%) | 17.5 | 47.0 | 0 | 1,177.7 |
| Distance (km) | 8,551.1 | 4,712.1 | 1 | 19,930.0 |
| Contiguous border | 0.01 | 0.1 | 0 | 1 |
| Common official language | 0.2 | 0.4 | 0 | 1 |

*Notes:* Inter- and intranational trade flows are reported in current million of U.S. dollars. Contiguous border and common official language are indicator variables equal to one if a country pair shares a border or an official language, respectively, and zero otherwise.

costs. About 1 percent of country pairs in the data share a border, while roughly 24 percent share a common official language.

# 4 Results

This section presents the main results. We first report our econometric estimates. We then present the results of our counterfactual simulation analysis.

## 4.1 Econometric Estimates

Table 3 reports the estimates of Equation (5) for each commodity. In line with expectations, the estimated values of the trade elasticity ($-\theta_k$) as identified through variation in tariffs ($\log(1 + t)$) are universally negative, highly elastic, and statistically significant, indicating that, on average, higher tariffs reduce bilateral trade. The magnitudes, however, vary substantially across commodities. Livestock products are generally more tariff-responsive than crops: the estimated elasticities for pork, chicken, and beef range from –6.049 to –13.288 and are relatively precisely estimated. For crops, values of the trade elasticity tend to be smaller in magnitude and less precisely estimated, ranging from –3.089 for soybeans to –7.886 for wheat. Overall, the results show that tariff barriers meaningfully diminish trade across all seven commodities, while also highlighting substantial heterogeneity in tariff responsiveness across products.[24]

The estimates on the gravity covariates, while not of central interest, largely behave as expected. Bilateral distance acts as a deterrent to trade, with estimates on this variable showing a strongly elastic negative relationship with bilateral trade across all commodities. Interestingly, contiguous borders are uniformly associated with reduced trade flows. Two factors help to understand this result. First, countries sharing contiguous borders tend to possess similar natural endowments;

[24]Our estimates of the trade elasticity for these commodities also align with comparable estimates from the literature. For instance, using a similar gravity-modeling approaching, Fontagné et al. (2022) estimate elasticities of –4.9 for beef (the average of their estimates for HS 0201 and 0202), –3.2 for poultry, –14.8 for pork, –3.6 for maize, –6.5 for rice, –6.2 for soybeans, and –2.6 for wheat.

**Table 3:** Estimates of Gravity Equation

| | Livestock Products | | | Crops | | | |
|---|---|---|---|---|---|---|---|
| | Beef | Chicken | Pork | Maize | Rice | Soybeans | Wheat |
| $\log(1+t)$ | $-6.049^{***}$ | $-9.702^{***}$ | $-13.288^{***}$ | $-6.983^{***}$ | $-7.208^{***}$ | $-3.089^{***}$ | $-7.886^{***}$ |
| | (0.581) | (0.825) | (1.348) | (2.361) | (2.570) | (1.073) | (1.006) |
| log(DIST) | $-2.573^{***}$ | $-2.732^{***}$ | $-2.894^{***}$ | $-2.757^{***}$ | $-2.790^{***}$ | $-2.672^{***}$ | $-2.845^{***}$ |
| | (0.137) | (0.162) | (0.108) | (0.101) | (0.144) | (0.183) | (0.089) |
| CNTG | $-1.231^{***}$ | $-1.083^{***}$ | $-1.101^{***}$ | $-1.862^{***}$ | $-1.630^{***}$ | $-1.986^{***}$ | $-2.202^{***}$ |
| | (0.141) | (0.164) | (0.149) | (0.332) | (0.238) | (0.634) | (0.347) |
| COMLANG | $0.579^{***}$ | $0.534^{**}$ | $0.878^{***}$ | $-2.117^{***}$ | $-0.136$ | $-1.115$ | $-0.532^{*}$ |
| | (0.181) | (0.220) | (0.171) | (0.566) | (0.186) | (1.733) | (0.275) |
| Observations | 889,391 | 895,482 | 800,381 | 623,839 | 656,653 | 442,873 | 511,110 |

*Notes:* Dependent variable in each regression is the value of unidirectional exports by commodity. Each estimation includes exporter–year and importer–year fixed effects. Robust standard errors clustered by bilateral pair reported in parentheses. *** $p < 0.01$, ** $p < 0.05$, * $p < 0.1$.

based on classical notions of comparative advantage, such countries will have less incentive to trade with one another relative to countries possessing considerably different endowment structures. Second, note that the estimates on this variable are conditional on bilateral distance and other controls. Considering this, the estimates on this variable reflect border effects net of the impact of geographical proximity already accounted for by the distance variable. Finally, the estimates on common language point to a scattered relationship between this variable and trade flows: for livestock products, common language is consistently associated with elevated trade volumes, while for crops, we find a negative (though generally weakly significant) relationship.

## 4.2 Counterfactual Experiments

With the econometric parameter estimates in hand, we next present the findings of our counterfactual simulation analysis. We organize our presentation of the simulation results around three main questions. First, we investigate the degree to which existing tariff preferences have influenced trade-embodied emissions relative to a world in which all preferential rates were reverted to MFN tariffs. Second, we explore trade and environmental outcomes in a hypothetical setting in which all existing tariff barriers are set to zero. Third, we assess how the different tariff regimes that we analyze shape the global distribution of trade-embodied GHG emissions by measuring the associated impacts on export-embodied emissions. For each counterfactual scenario, we report results separately for livestock products and crops, distinguishing between export- and import-embodied emissions.

#### First Scenario: Preferential vs. MFN

The country-specific results for the first counterfactual scenario are shown in Figures 4 and 5. In presenting the country-level estimates, we show the results for the twenty countries registering the largest absolute changes in trade-embodied emissions. The corresponding percentage changes relative to the baseline are reported in square brackets following the country names. The results show that trade-embodied emissions are generally higher under the observed applied-tariff regime than under the MFN benchmark. In aggregate, existing tariff preferences are estimated to increase annual global trade-embodied emissions by an estimated 37.9 Mt of $CO_2e$.[25] Valued at the current EU CBAM certificate price, this increase corresponds to an implied annual carbon value of approximately $3.4 billion. Livestock products account for 29.8 Mt of this increase, while crops account for 8.1 Mt, corresponding to implied annual carbon values of approximately $2.7 billion and $0.7 billion, respectively.

**Livestock Products.** The aggregate increase is driven primarily by livestock products, which account for nearly four-fifths of the total effect. We therefore begin with livestock before turning to crops. Figure 4 shows that tariff preferences have increased livestock-related embodied emissions mainly through beef trade. France is the largest exporter of tariff-preference-induced embodied emissions, with an increase of roughly 4,250 kt of $CO_2e$, more than 3,500 kt of which come from beef. France also ranks second-largest in terms of increased imports of embodied emissions. Relative to the MFN counterfactual, its export- and import-embodied emissions are 63.7% and 32.4% higher, respectively, under the observed preferential-tariff regime.

The prominence of countries such as France, Germany, Italy, and Spain points to the role of intra-EU tariff preferences in shaping trade in livestock products. Replacing preferential rates with MFN tariffs would reduce intra-EU trade volumes and lower the emissions embodied in those flows. Outside Europe, the United States appears as both a major importer and exporter, with a combined change exceeding 5,500 kt of $CO_2e$. This result for the United States is associated with tariff preferences established under the country's free trade agreements with large trade partners including Canada and Mexico, in addition to several bilateral agreements with partners such as Japan and South Korea and the plurilateral Central American Free Trade Agreement.

Several Southeast Asian countries, including Vietnam, Thailand, and Indonesia, also exhibit sizable increases on both sides of trade. These countries are party to multiple preferential trading arrangements, such as the Association of Southeast Asian Nations trade agreement, whose tariff preferences contribute to elevated levels of trade. In addition, livestock production in these countries—which is primarily water buffalo rather than cattle—is generally highly emissions-intensive. For instance, as of 2022, Indonesia's livestock production for meat was associated with

[25] The estimated 37.9 Mt of $CO_2e$ corresponds to 31.7 kt of $N_2O$ and 1,053.9 kt of $CH_4$. This estimate is based on the GWP factors reported in the fifth IPCC assessment report. The most recent GWP factors from the sixth IPCC assessment report imply a total increase of about 38.1 Mt of $CO_2e$.

**Figure 4:** Estimated Differences in Trade-Embodied Emissions for Livestock Products, Preferential vs. MFN Scenario

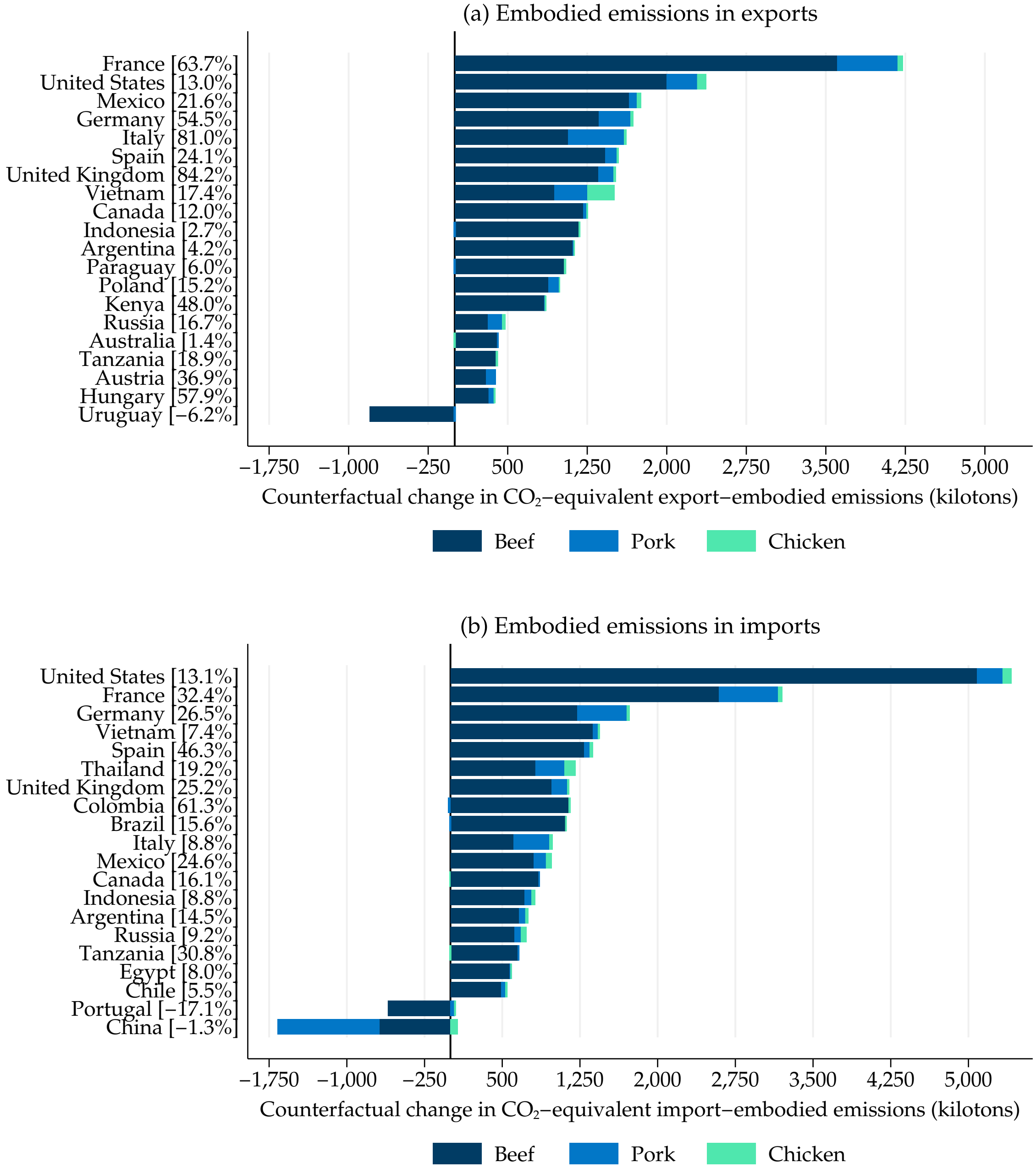


*Notes:* Figure reports the difference in $CO_2$e emissions embodied in livestock-product trade between the observed preferential-tariff regime and the MFN counterfactual for the year of analysis (2022) and the twenty countries registering the largest estimated absolute change in embodied emissions. Panel (a) shows export-embodied emissions, while panel (b) shows import-embodied emissions. Positive values indicate that embodied emissions are higher under the observed preferential-tariff regime than under the MFN benchmark. Corresponding percentage changes relative to the baseline are reported in square brackets.

emissions intensities of 64.7 kilograms (kg) of $CO_2$ equivalent per kg of production, substantially higher than the corresponding global average of 30.5 kg of $CO_2$ equivalent per kg (based on data from FAO). This highlights that the results are driven not only by the extent to which tariff preferences bolster trade, but by the emission intensities of the countries whose exports are influenced by these preferences.

A small number of countries move in the opposite direction. Uruguay's beef exports, Portugal's beef imports, and China's beef and pork imports decline under the observed preferential-tariff regime relative to the MFN benchmark. These declines are consistent with trade diversion: countries receiving smaller preference margins lose relative competitiveness as trade is directed toward partners benefiting from larger tariff reductions in the baseline scenario.

**Crops.** Figure 5 shows the corresponding results for crop products. In contrast to livestock, where beef dominates the emissions response, crop-related changes are concentrated primarily in rice. This reflects both the scale of rice trade and its relatively high emission intensity within the crop group.

China accounts for the largest changes in crop-related embodied emissions due to existing tariff preferences, with $CO_2e$ increases of about 2,873 kt on the export side and 2,933 kt on the import side. Other Asian countries also feature prominently, especially South Korea and Japan, with changes driven largely by rice trade. The concentration of these effects is striking: the three countries with the largest estimated impacts on embodied emissions account for more than two-thirds of the total simulated change in both export- and import-embodied emissions. Several African countries, including Nigeria, Tanzania, and Benin, also engage in significantly higher levels of exports due to the observed preferential-tariff regime.

A small number of countries register decreases in embodied emissions under the preferential-tariff regime relative to the MFN benchmark. Togo, Venezuela, and Uganda, for example, exhibit declines in import-embodied emissions. This pattern is consistent with trade diversion: these destinations appear to benefit less from preferential tariff reductions than other markets, causing trade to shift elsewhere and reducing the emissions embodied in their imports.

The results from the first counterfactual experiment deliver a clear message: existing tariff preferences have raised the emissions embodied in agricultural trade, mainly by expanding trade in emission-intensive products such as beef and rice and shifting exports towards emission-intensive producers. The effects are highly concentrated across countries, reflecting the fact that preferential access changes not only the volume of trade but also the geography of production.

### Second Scenario: Complete Trade Liberalization

Figures 6 and 7 report the results for the second counterfactual experiment, in which bilateral tariffs are set to zero globally. As before, the plotted values are measured as the baseline value mi-

**Figure 5:** Estimated Differences in Trade-Embodied Emissions for Crops, Preferential vs. MFN Scenario

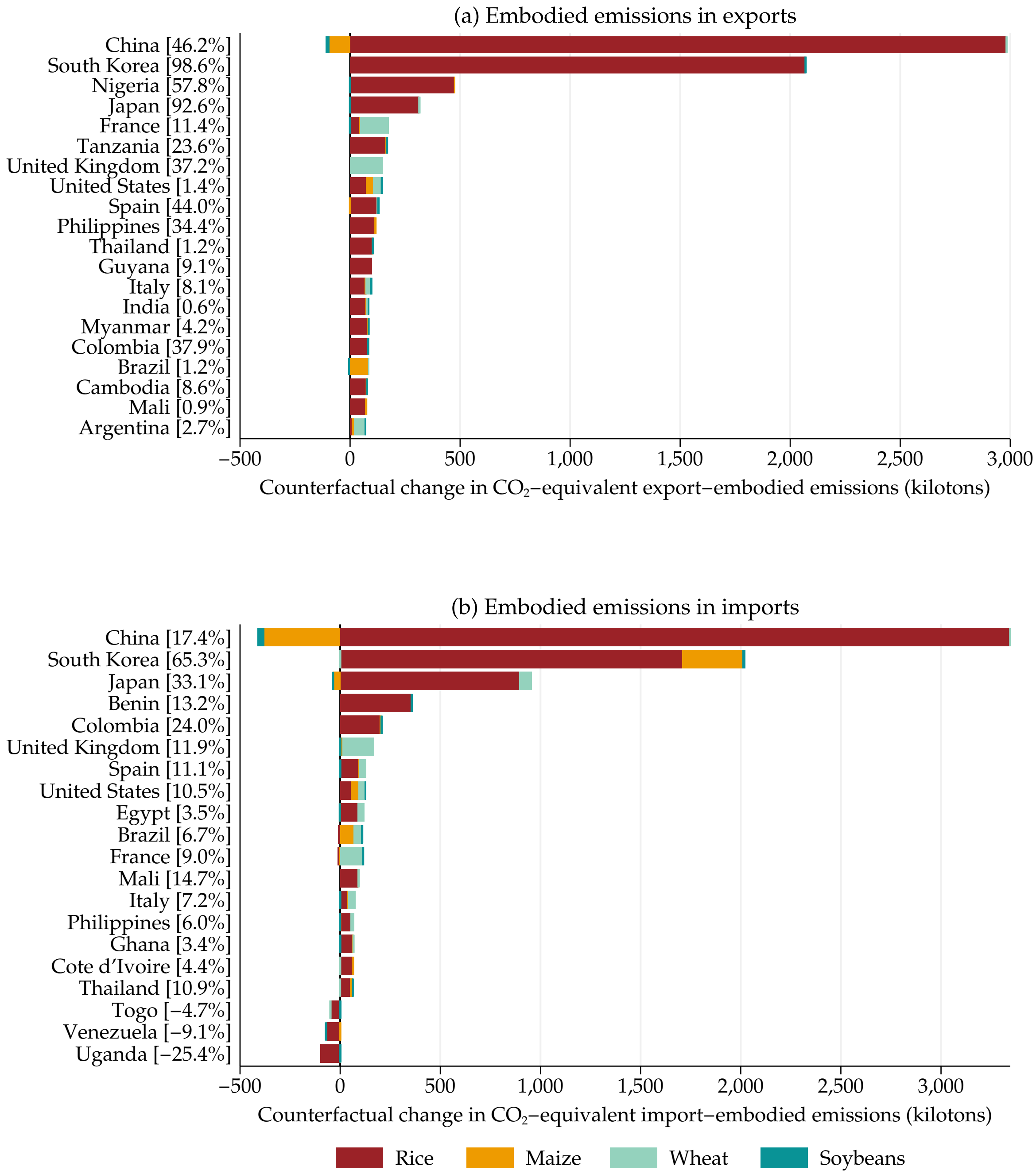


*Notes:* Figure reports the difference in $CO_2$e emissions embodied in crop trade between the observed preferential-tariff regime and the MFN counterfactual for the year of analysis (2022) and the twenty countries registering the largest estimated absolute change in embodied emissions. Panel (a) shows export-embodied emissions, while panel (b) shows import-embodied emissions. Positive values indicate that embodied emissions are higher under the observed preferential-tariff regime than under the MFN benchmark. Corresponding percentage changes relative to the baseline are reported in square brackets.

nus the counterfactual value. Positive values therefore identify cases for which full liberalization would *reduce* embodied emissions, while negative values identify cases for which it would *increase* embodied emissions. In aggregate, removing all remaining tariffs increases trade-embodied emissions by approximately 17.7 Mt of $CO_2e$, corresponding to an implied annual carbon value of approximately \$1.6 billion at the EU CBAM certificate price.[26] Crops account for 12.1 Mt of this increase, while livestock products account for 5.6 Mt, equivalent to approximately \$1.1 billion and \$0.5 billion, respectively. In presenting the results for this analysis, we again report the results only for the twenty countries with the largest estimated absolute changes.

**Livestock Products.** Figure 6 shows that expected adjustments in trade-embodied emissions attributable to removing all remaining tariffs in livestock products are dominated by beef, as in the first scenario. However, the pattern of impacts across countries differs markedly from the earlier counterfactual. In the first experiment, the largest effects for livestock products were concentrated among countries whose trade is strongly shaped by existing preferential access, including France, the United States, Mexico, and several other EU member states. Under full liberalization, the ranking becomes more dispersed. Some countries that were central in the first experiment become less prominent, while a different set of exporters and importers emerges once all existing tariff barriers are removed.

On the export side, the results for which are shown in panel (a) of Figure 6, full liberalization reduces export-embodied emissions for several established beef exporters, such as Australia and Poland. This suggests that their current export patterns partly reflect market-access advantages that weaken when all suppliers face zero tariffs. The United States provides a useful example of this reshuffling. Although it played a major role in the first counterfactual, it no longer appears among the top twenty exporter-side changes under full liberalization. This reflects offsetting movements across destinations: exports fall to markets that already grant favorable access under the current status quo, such as South Korea, Japan, and Mexico, and expand to markets where existing applied tariffs are higher, such as China and the European Union.

At the same time, full liberalization shifts export opportunities toward a different set of countries. Iran, Ethiopia, Turkey, Myanmar, Brazil, and Argentina see higher export-embodied emissions under the zero-tariff counterfactual, suggesting that the current global tariff regime imposes a significant constraint on their exports of livestock products. Once existing tariff barriers are removed, these countries register an expanded role in global trade, increasing the emissions embodied in their exports.

In addition, the set of livestock products that undergo sizable impacts becomes broader. Beef remains dominant, but embodied emissions in chicken are significantly affected for countries such as Iran, Turkey and Pakistan. The main lesson is that full liberalization does not simply mag-

[26] Using the first-quarter 2026 CBAM certificate price of \$89.64 per tonne of $CO_2e$, 17.7 Mt $CO_2e$ corresponds to approximately \$1.6 billion.

**Figure 6:** Estimated Differences in Trade-Embodied Emissions for Livestock Products, Complete Trade Liberalization Scenario

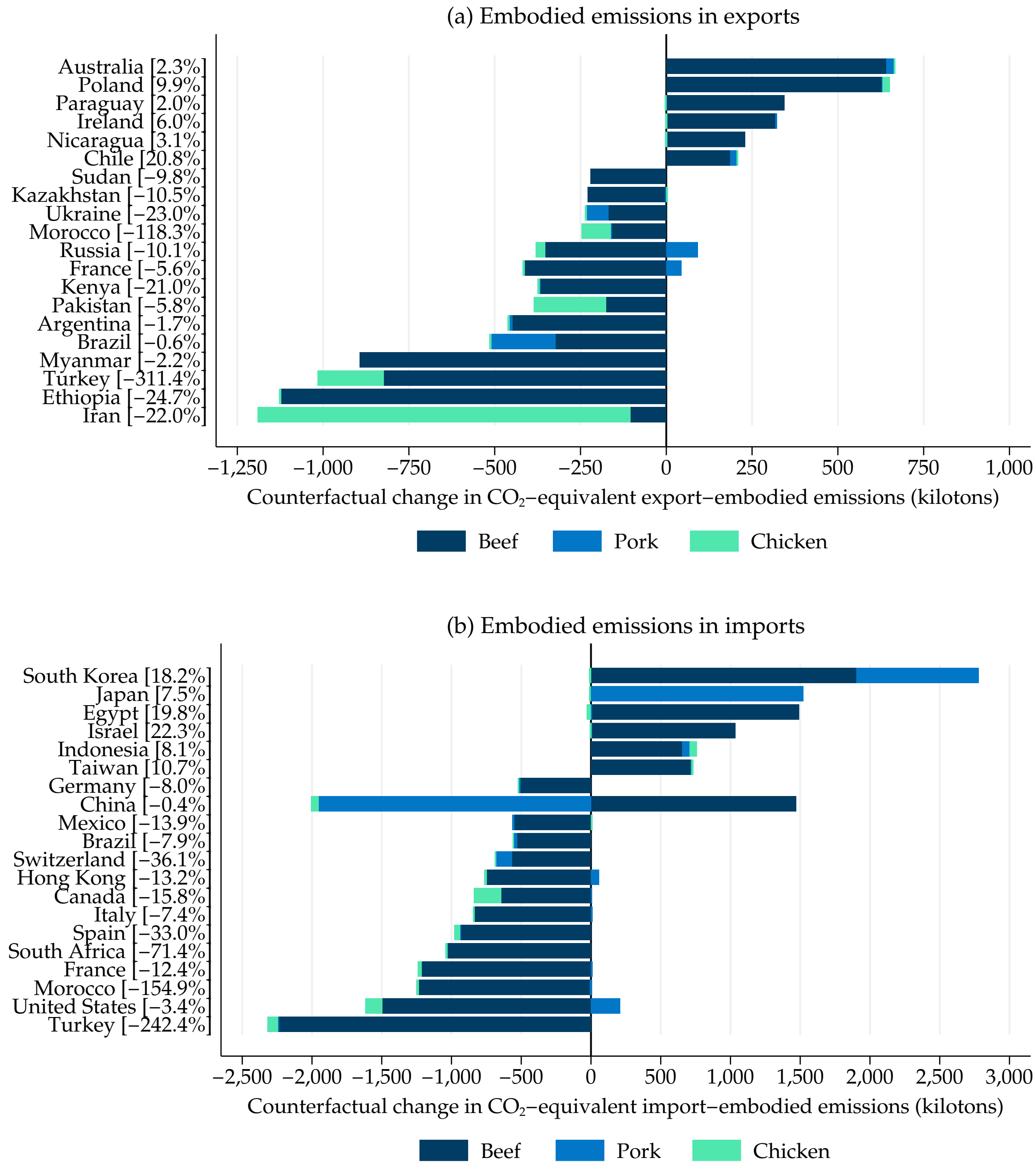


*Notes:* Figure reports the difference in $CO_2$e emissions embodied in livestock-product trade between the observed tariff regime and a zero-tariff counterfactual for the year of analysis (2022) and the twenty countries registering the largest estimated absolute change in embodied emissions. Panel (a) shows export-embodied emissions, while panel (b) shows import-embodied emissions. Positive values indicate that embodied emissions are higher under the observed tariff regime than under full liberalization; negative values indicate that full liberalization would increase embodied emissions. Corresponding percentage changes relative to the baseline are reported in square brackets.

nify the patterns observed under the MFN counterfactual with respect to countries and products. Indeed, the results from this scenario display notable differences in terms of both countries and products driving the emissions response.

Panel (b) of Figure 6 shows that the importer-side response also deviates significantly from the results of the earlier scenario. The United States remains important in both exercises, but the direction and scale of the adjustment change under the zero-tariff counterfactual. In the first experiment, existing tariff preferences are estimated to raise U.S. import-embodied emissions. Under full liberalization, by contrast, U.S. import-embodied emissions fall, suggesting that removing all remaining tariff barriers reallocates sourcing in a way that reduces the emissions embodied in its imports of livestock products.

South Korea and Japan—two countries that maintain high tariffs on agricultural imports—illustrate a different margin. The results for these countries do not rank among the largest importer-side changes in the preferential-to-MFN experiment, but they become central under full liberalization. This suggests that these countries' import patterns are shaped less by existing tariff preferences and more by the tariff barriers that still remain under the current regime. Once these barriers are removed, sourcing is reorganized in a way that lowers their import-embodied emissions on net. China displays a more product-specific response: its adjustment differs across livestock products, with pork and beef moving along distinct margins, so the aggregate effect masks offsetting changes across commodities. Taken together, these importer-side results reinforce the broader message from the analysis of exports: full liberalization does not simply magnify the pattern revealed by the preferential-to-MFN counterfactual. Rather, it reveals different country- and product-level margins of trade and emissions reallocations.

**Crops.** Figure 7 shows that the response for embodied emissions in crop trade under full liberalization is even more concentrated than in the preferential-to-MFN counterfactual and is dominated by rice. In the first experiment, tariff preferences increased crop-related embodied emissions mainly through a small set of Asian countries, especially China, Japan, and South Korea. Under the zero-tariff counterfactual, the same region remains central, but the scale and direction of the adjustment change sharply. China, South Korea, the Philippines, Japan, and India all register higher export-embodied emissions under full liberalization, indicating that existing tariff barriers substantially constrain these countries' exports of several major crops.

The cases of rice-related embodied emissions for Japan and South Korea help to illustrate why the full-liberalization experiment is not just a mechanical extension of the MFN counterfactual. Existing preferences already make these countries central to embodied emissions in rice trade, but rice remains a highly protected product: a large share of rice trade takes place under MFN tariffs, and faces high levels of protectionism in many large markets. Consequently, for countries such as Japan and South Korea, a reduction from the currently high levels of effective protection from imports to zero tariffs translates into large changes in export- and import-embodied emissions.

**Figure 7:** Estimated Differences in Trade-Embodied Emissions for Crops, Complete Trade Liberalization Scenario

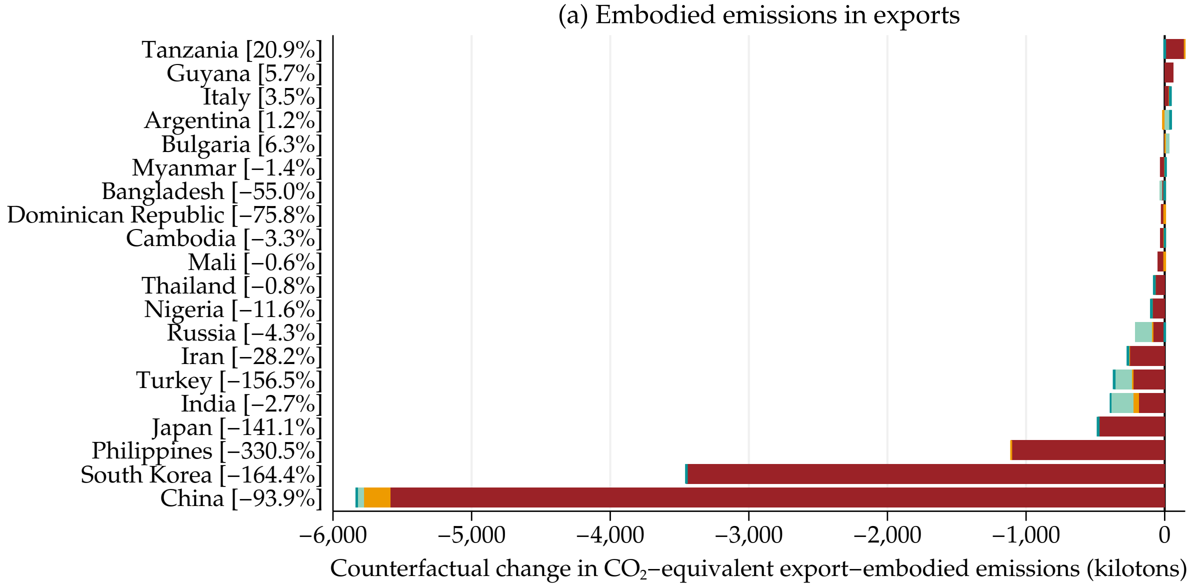


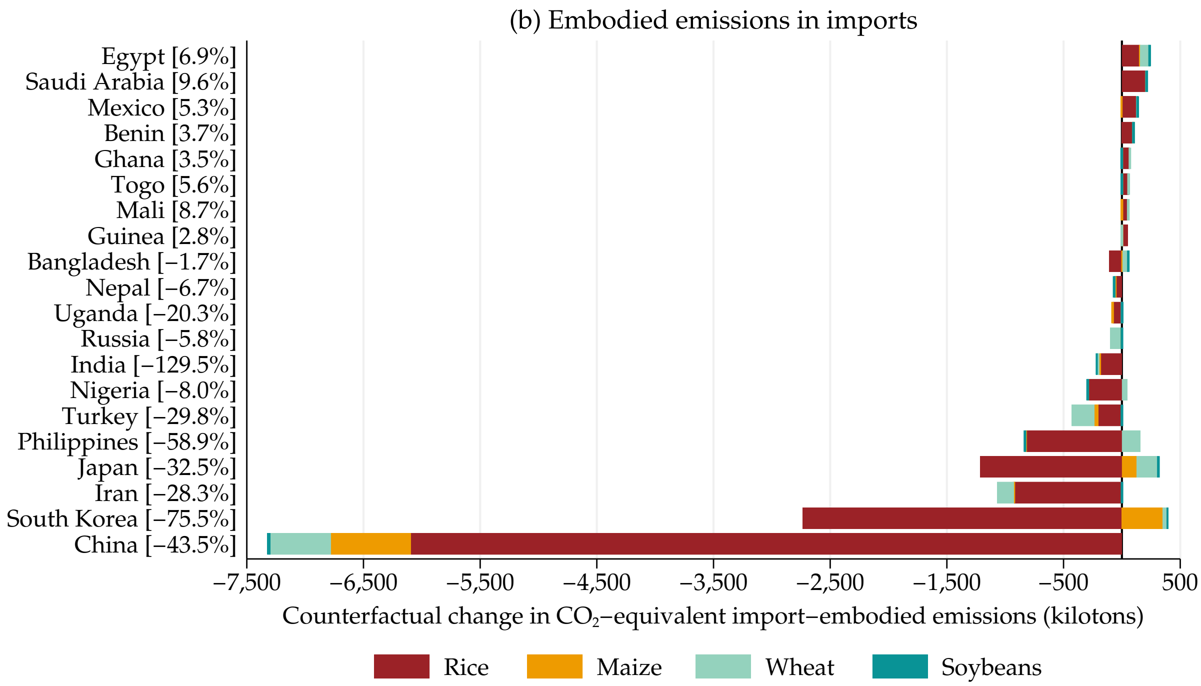


*Notes:* Figure reports the difference in $CO_2$e emissions embodied in crop trade between the observed tariff regime and a zero-tariff counterfactual for the year of analysis (2022) and the twenty countries registering the largest estimated absolute change in embodied emissions. Panel (a) shows export-embodied emissions, while panel (b) shows import-embodied emissions. Positive values indicate higher embodied emissions under the observed regime; negative values indicate higher embodied emissions under full liberalization. Corresponding percentage changes relative to the baseline are reported in square brackets.

**Figure 8:** Tariff Liberalization and the Global Geography of Embodied Emissions

(a) Preferential vs. MFN

(b) Complete Trade Liberalization

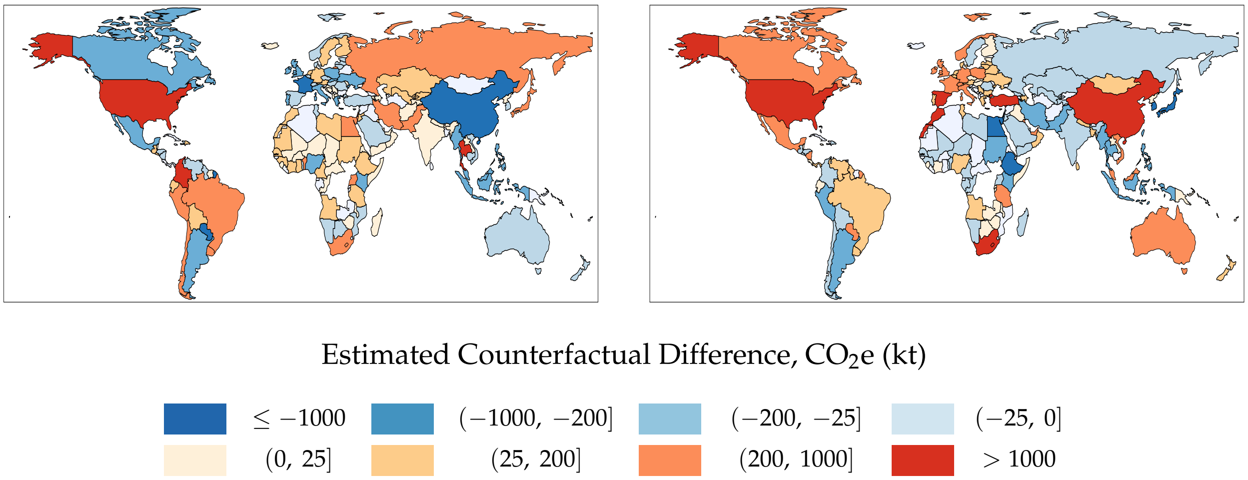


*Notes:* For each country, net changes are calculated as the change in export-embodied emissions minus the change in import-embodied emissions. Panel (a) illustrates the transition from MFN tariffs to preferential tariff rates, while panel (b) illustrates the transition from preferential tariffs to full liberalization. Red shades identify countries with increases in net export-embodied emissions under the respective counterfactuals, while blue shades indicate those with increases in net import-embodied emissions. Darker shades indicate larger changes in the corresponding direction. Color bins are defined based on quartile cutoffs of the empirical distribution.

**The Global Geography of Tariff-Induced Embodied Emissions**

The preceding results illuminate how tariff counterfactuals shape embodied emissions across countries and products separately for exports and imports. Figure 8 provides a complementary view by summarizing these changes at the country level in terms of net embodied-emission positions. It specifically shows which countries become larger net sources of embodied emissions and which become larger net destinations, offering a systematic view of how tariff liberalization redirects the emissions embodied in agricultural trade.

Panel (a) shows the geography of the differences implied by changing from MFN tariffs to the preferential tariff rates observed in the current regime. Under this margin of liberalization, net export-embodied emissions increase in several major agricultural exporters, such as Brazil, Thailand, and the United States, while net import-embodied emissions increase in countries such as Australia, Canada, and China. This pattern is consistent with the earlier results showing that existing tariff preferences have expanded trade in emission-intensive products, but that the resulting emissions are concentrated in particular country–product relationships rather than distributed evenly across the world.

Panel (b) depicts the spatial distribution of counterfactual impacts when all existing tariff barriers are removed. As explained earlier, the zero-tariff scenario does not simply extend the pattern generated by the preferential-to-MFN experiment. In contrast with the results in panel (a), some countries identified as net importers under the first scenario become net exporters under the second scenario, while others move in the opposite direction. This contrast reinforces the central point of the second counterfactual scenario: the current global tariff regime reflects both preferential liberalization that has already occurred and existing barriers that continue to constrain trade. Removing those remaining barriers activates a different set of country-product margins.

The patterns captured by Figure 8 should be interpreted as a summary of geographical incidence rather than as a complete description of gross trade flows. A country classified as a net importer of embodied emissions may attain that position because import-embodied emissions rise more than export-embodied emissions, but it may also do so because export-embodied emissions fall more than import-embodied emissions. Similarly, a country appearing as a net exporter may experience increases on both sides of trade, with the export-side change dominating. Thus, countries in the same color category may arrive there through different underlying adjustments. The map is therefore most informative when read together with the export- and import-side results above.

In summary, Figure 8 shows that tariff liberalization reshapes not only the volume of agricultural trade but also the global distribution of emissions embodied in that trade. The geography as determined by preferential tariff reductions differs sharply from the geography implied by removing all remaining tariffs. This distinction matters for policy: evaluating the environmental consequences of trade liberalization requires knowing not only whether trade expands, but which countries become larger net sources or destinations of embodied emissions, and through which commodities those changes occur.

Finally, to summarize the estimated total impacts on the embodied GHG content of trade identified across the two scenarios, Table 4 presents the results on aggregate GHG content across the seven commodities for the two counterfactual scenarios, broken down by $CH_4$, $N_2O$, and the implied $CO_2$ equivalent that cumulates the total estimated impacts across both $CH_4$ and $N_2O$. The estimates in the table reaffirm the findings elaborated above. In particular, the results from both scenarios confirm that a handful of commodities account for the bulk of trade policy-induced embodied GHG emissions from agriculture: in order of the magnitude of implied embodied emissions content, these commodities include beef, rice, pork, chicken, and wheat. Additionally, existing tariff preferences and the current global system of import tariffs more broadly are important determinants of the emissions footprint of international agricultural trade, as evidenced by the substantial influence exerted by different tariff regimes on the international geography of farm-gate emissions.

Taken together, our findings show that existing tariff preferences increase global trade-embodied emissions by about 37.9 Mt of $CO_2$e for the commodities in the analysis. By contrast, the scenario considering global free trade shows that setting all existing tariffs to zero would cause global

**Table 4:** Estimated Counterfactual Changes in Trade-Embodied Emissions for $CH_4$, $N_2O$, and $CO_2e$ by Commodity and Scenario

| | First Scenario: Preferential vs. MFN Tariffs | | | Second Scenario: Complete Trade Liberalization | | |
|---|---|---|---|---|---|---|
| Commodity | $CH_4$ | $N_2O$ | $CO_2e$ | $CH_4$ | $N_2O$ | $CO_2e$ |
| Beef | 714.7 | 20.7 | 25,497.1 | –105.9 | –4.2 | –4,078.2 |
| Chicken | 5.3 | 3.4 | 1,049.4 | –10.0 | –6.5 | –2,002.5 |
| Pork | 89.8 | 2.7 | 3,229.9 | 18.3 | –0.2 | 459.4 |
| Maize | 1.0 | 0.3 | 107.5 | –1.8 | –0.6 | –209.4 |
| Rice | 240.4 | 1.7 | 7,181.7 | –385.5 | –2.8 | –11,536.0 |
| Soybeans | 0.0 | 0.04 | 10.6 | 0.0 | –0.03 | –7.95 |
| Wheat | 2.8 | 2.9 | 846.9 | –1.5 | –1.1 | –333.5 |
| Total | 1,053.9 | 31.7 | 37,923.1 | –486.3 | –15.4 | –17,708.2 |

*Notes:* Emissions changes are measured in kt. Following the sign convention throughout the paper, the negative signs in the results for the second scenario indicate an increase in embodied emissions. $CO_2e$ is computed as the sum of the corresponding $CO_2e$ values for $CH_4$ and $N_2O$ calculated using GWP values of 28 for $CH_4$ and 265 for $N_2O$.

trade-embodied emissions to rise by around 17.7 Mt of $CO_2e$. These totals are modest relative to the total annual level of global farm-gate $CH_4$ and $N_2O$ emissions, which amounted to 7,966.4 Mt of $CO_2e$ in 2022 (FAO, 2024a). Nonetheless, our results point to a non-trivial role played by trade policy in shaping the GHG emissions generated by the agricultural sector.

# 5 Conclusion

We study how tariff policy determines the GHG emissions embodied in agricultural trade. Trade barriers such as tariffs shape the patterns of production and sourcing across countries, and countries differ in the farm-gate emission intensity with which they produce the same commodities. We quantify these relationships by combining a structural gravity estimation and simulation modeling approach with information on applied tariffs and country–commodity-specific $CH_4$ and $N_2O$ emission intensities for seven major agricultural commodities.

The results show that tariff policy meaningfully shapes the emissions content of agricultural trade. Existing tariff preferences increase global trade-embodied farm-gate emissions by about 37.9 Mt of $CO_2e$, with livestock products, especially beef, accounting for most of the increase and rice driving much of the crop-related response. A zero-tariff counterfactual reveals a different margin of adjustment: removing all remaining tariffs increases trade-embodied emissions by about 17.7 Mt of $CO_2e$, but through a different set of country-product reallocations rather than by simply magnifying the pattern generated by existing preferences. Together, the two experiments show that the current tariff system matters through two margins: preferential liberalization already embedded in applied tariffs and residual tariff barriers that continue to constrain trade.

The interpretation of these estimates should be tied to the scope of the exercise. We focus on farm-gate $CH_4$ and $N_2O$ because these gases are central to agriculture's climate footprint and can be systematically linked to country–commodity-level production and trade flows across a large set of countries. Similarly, our focus on seven primary commodities reflects a trade-off between coverage and measurement consistency. The analysis does not include downstream processing, upstream input production, transportation, land-use change, or endogenous changes in emission intensities. These margins could amplify or dampen the effects we quantify; however, incorporating them would require comprehensive data that systematically trace production responses beyond average country–commodity farm-gate emission intensities. Our estimates should therefore be read as structural trade-policy simulations evaluated at observed average farm-gate emission intensities, rather than full life-cycle or welfare calculations.

The broader implication of our analysis is that the environmental consequences of trade policy depend on the geography of production, not simply on the volume of trade. Changes in trade barriers can raise or lower embodied emissions depending on which products see expanded trade and production, which countries gain or lose market share, and how emission intensities vary across source countries. Trade policy is not a stand-alone climate instrument, but it can reinforce or mitigate environmental externalities by changing where production and sourcing occur. This points to the importance of environmental comparative advantage: the social cost of producing the same agricultural commodity can differ sharply across countries, and trade policy plays an active role in determining whether global production shifts toward or away from lower-emission sources.

Our results are informative about possible avenues of future research. Future work could incorporate broader life-cycle emissions, allow emission intensities to adjust endogenously, or evaluate emissions-indexed trade policies such as border levies tied to country–commodity emission intensities. The central message, however, is already clear: trade policy is an important factor in shaping the environmental consequences of global trade.

# References


Aichele, R. and Felbermayr, G. (2015). Kyoto and carbon leakage: An empirical analysis of the carbon content of bilateral trade. *Review of Economics and Statistics*, 97(1):104–115.

Anderson, J., Larch, M., and Yotov, Y. (2018). GEPPML: General equilibrium analysis with PPML. *The World Economy*, 41(10):2750–2782.

Anderson, J. and van Wincoop, E. (2003). Gravity with gravitas: A solution to the border puzzle. *American Economic Review*, 93(1):170–192.

Anderson, J. and van Wincoop, E. (2004). Trade costs. *Journal of Economic Literature*, 42(3):691–751.

Barrozo, M. (2024). Where is the beef? Supply chains and carbon emissions in the Amazon. Working paper, DePaul University.

Bruckner, M., Giljum, S., Lutz, C., and Svenja Wiebe, K. (2012). Materials embodied in international trade – Global material extraction and consumption between 1995 and 2005. *Global Environmental Change*, 22(3):568–575.

Chen, B., Li, J., Wu, X., Han, M., Zeng, L., Li, Z., and Chen, G. (2018). Global energy flows embodied in international trade: A combination of environmentally extended input–output analysis and complex network analysis. *Applied Energy*, 210:98–107.

Costinot, A., Donaldson, D., and Smith, C. (2016). Evolving comparative advantage and the impact of climate change in agricultural markets: Evidence from 1.7 million fields around the world. *Journal of Political Economy*, 124(1):205–248.

Dadakas, D., Pitoňáková, R., and Ioannidis, E. (2025). The impact of the Crimea annexation on agricultural trade: A structural gravity approach. *European Review of Agricultural Economics*, 52(3):531–566.

Fally, T. (2015). Structural gravity and fixed effects. *Journal of International Economics*, 97(1):76–85.

FAO (2023). Pathways towards lower emissions: A global assessment of the greenhouse gas emissions and mitigation options from livestock agrifood systems. Technical report, Food and Agriculture Organization of the United Nations, Rome.

FAO (2024a). FAOSTAT Climate Change: Agrifood systems emissions, Emissions from crops. Food and Agriculture Organization of the United Nations. Available at `http://www.fao.org/faostat/en/#data/GCE`. Accessed October 14th, 2024.

FAO (2024b). FAOSTAT Statistical Database. Food and Agriculture Organization of the United Nations. Available at `http://www.fao.org/faostat/en/#data`. Accessed October 14th, 2024.

Fontagné, L., Guimbard, H., and Orefice, G. (2022). Tariff-based product-level trade elasticities. *Journal of International Economics*, 137:103593.

Garnett, T. (2011). Where are the best opportunities for reducing greenhouse gas emissions in the food system (including the food chain)? *Food Policy*, 36:S23–S32.

Gaulier, G. and Zignago, S. (2010). BACI: International trade database at the product-level. Munich Personal RePEc Archive Paper No. 31398.

Gouel, C. and Laborde, D. (2021). The crucial role of domestic and international market-mediated adaptation to climate change. *Journal of Environmental Economics and Management*, 106:102408.

Gurevich, T. and Herman, P. (2018). The Dynamic Gravity Dataset: 1984–2016. USITC Working Paper No. 2018-02-A.

Hong, C., Burney, J., Pongratz, J., Nabel, J., Mueller, N., Jackson, R., and Davis, S. (2021). Global and regional drivers of land-use emissions in 1961–2017. *Nature*, 589(7843):597–603.

Hong, C., Zhao, H., Qin, Y., Burney, J., Pongratz, J., Hartung, K., Liu, Y., et al. (2022). Land-use emissions embodied in international trade. *Science*, 376(6593):597–603.

Hultgren, A., Carleton, T., Delgado, M., Gergel, D., Greenstone, M., Houser, T., Hsiang, S., Jina, A., Kopp, R. E., Malevich, S., et al. (2025). Impacts of climate change on global agriculture accounting for adaptation. *Nature*, 642(8068):644–652.

Johnson, J., Franzluebbers, A., Lachnicht Weyers, S., and Reicosky, D. (2007). Agricultural opportunities to mitigate greenhouse gas emissions. *Environmental Pollution*, 150(1):107–124.

Larch, M., Luckstead, J., and Yotov, Y. (2024). Economic sanctions and agricultural trade. *American Journal of Agricultural Economics*, 106(4):1477–1517.

Li, M., Jia, N., Lenzen, M., Malik, A., Wei, L., Jin, Y., and Raubenheimer, D. (2022). Global food-miles account for nearly 20% of total food-systems emissions. *Nature Food*, 3(6):445–453.

Lichtenberg, E. (2002). Chapter 23: Agriculture and the environment. In *Handbook of Agriculture Economics Vol. 2 Part A*, B. Gardner and G. Rausser (eds.). Amsterdam: North-Holland.

Liu, L.-J., Creutzig, F., Yao, Y.-F., Wei, Y.-M., and Liang, Q.-M. (2020). Environmental and economic impacts of trade barriers: The example of China–US trade friction. *Resource and Energy Economics*, 59:101144.

Luckstead, J. (2022). Impacts of bilateral trade agreements between the United States and Latin American countries on agri-food trade. *Journal of Agricultural and Resource Economics*, 47(3):673–696.

Nabuurs, G.-J., Mrabet, R., Abu Hatab, A., Bustamante, M., Clark, H., Havlík, P., House, J., Mbow, C., Ninan, K., Popp, A., et al. (2022). Agriculture, forestry and other land uses (AFOLU). 2022: Agriculture, Forestry and Other Land Uses (AFOLU). In IPCC, 2022: *Climate Change 2022: Mitigation of Climate Change. Contribution of Working Group III to the Sixth Assessment Report of the Intergovernmental Panel on Climate Change*, P.R. Shukla, J. Skea, R. Slade, A. Al Khourdajie, R. van Diemen, D. McCollum, M. Pathak, S. Some, et al. (eds.).

Nath, I. (2025). Climate change, the food problem, and the challenge of adaptation through sectoral reallocation. *Journal of Political Economy*, 133(6):1705–1756.

Pachauri, R., Allen, M., Barros, V., Broome, J., Cramer, W., Christ, R., Church, J., Clarke, L., Dahe, Q., Dasgupta, P., et al. (2014). *Climate change 2014: Synthesis report. Contribution of Working Groups I, II and III to the fifth assessment report of the Intergovernmental Panel on Climate Change*. IPCC.

Park, D., Howard, J., and Ridley, W. (2024). Regional heterogeneity in environmental quality: The role of firm production networks and trade. *Journal of the Association of Environmental and Resource Economists*, 11(5):1311–1349.

Park, D. and Ridley, W. (2025). Thirsty for trade: How globalization shapes virtual water trade. *Environmental and Resource Economics*, 88(2):279–338.

Ridley, W. and Devadoss, S. (2023). Competition and trade policy in the world cotton market: Implications for US cotton exports. *American Journal of Agricultural Economics*, 105(5):1365–1387.

Ridley, W. and Shirin, F. (2025). The effectiveness of development-oriented non-reciprocal trade preferences in promoting agricultural trade. *American Journal of Agricultural Economics*, 107(1):81–107.

Santos Silva, J. and Tenreyro, S. (2006). The log of gravity. *Review of Economics and Statistics*, 88(4):641–658.

Shapiro, J. (2016). Trade costs, $CO_2$, and the environment. *American Economic Journal: Economic Policy*, 8(4):220–254.

Shapiro, J. (2021). The environmental bias of trade policy. *Quarterly Journal of Economics*, 136(2):831–886.

Teti, F. (2024). Missing tariffs. CESifo Working Paper Series 11590.

Verburg, R., Stehfest, E., Woltjer, G., and Eickhout, B. (2009). The effect of agricultural trade liberalization on land-use related greenhouse gas emissions. *Global Environmental Change*, 19(4):434–446.

Vermeulen, S., Campbell, B., and Ingram, J. (2012). Climate change and food systems. *Annual Review of Environment and Resources*, 37:195–222.

World Bank (2025). World Integrated Trade Solutions (WITS) Database. Available at `https://wits.worldbank.org/`.

Xu, X., Sharma, P., Shu, S., Lin, T.-S., Ciais, P., Tubiello, F. N., Smith, P., Campbell, N., and Jain, A. K. (2021). Global greenhouse gas emissions from animal-based foods are twice those of plant-based foods. *Nature Food*, 2(9):724–732.

Xu, Y. and Dietzenbacher, E. (2014). A structural decomposition analysis of the emissions embodied in trade. *Ecological Economics*, 101:10–20.

Yotov, Y. (2022). On the role of domestic trade flows for estimating the gravity model of trade. *Contemporary Economic Policy*, 40(3):526–540.

# Appendix

**Table A1:** List of Countries in the Analysis

| | | |
|---|---|---|
| Afghanistan | Gabon | Pakistan |
| Albania | Gambia | Palau |
| Algeria | Georgia | Palestine |
| Angola | Germany | Panama |
| Antigua and Barbuda | Ghana | Papua New Guinea |
| Argentina | Greece | Paraguay |
| Armenia | Grenada | Peru |
| Aruba | Guatemala | Philippines |
| Australia | Guinea | Poland |
| Austria | Guinea-Bissau | Portugal |
| Azerbaijan | Guyana | Qatar |
| Bahamas | Haiti | Romania |
| Bahrain | Honduras | Russia |
| Bangladesh | Hong Kong | Rwanda |
| Barbados | Hungary | Samoa |
| Belarus | Iceland | Saudi Arabia |
| Belgium | India | Senegal |
| Belize | Indonesia | Serbia |
| Benin | Iran | Seychelles |
| Bermuda | Ireland | Sierra Leone |
| Bhutan | Israel | Singapore |
| Bolivia | Italy | Slovakia |
| Bosnia and Herzegovina | Jamaica | Slovenia |
| Botswana | Japan | Solomon Islands |
| Brazil | Jordan | South Africa |
| Brunei | Kazakhstan | South Korea |
| Bulgaria | Kenya | South Sudan |
| Burkina Faso | Kuwait | Spain |
| Burundi | Kyrgyzstan | Sri Lanka |
| Cabo Verde | Laos | St. Lucia |
| Cambodia | Latvia | St. Vincent and Grenadines |
| Cameroon | Lebanon | Sudan |
| Canada | Lesotho | Suriname |
| Cayman Islands | Liberia | Swaziland |
| Central African Republic | Libya | Sweden |
| Chad | Lithuania | Switzerland |
| Chile | Luxembourg | Syria |
| China | Macau | Taiwan |
| Colombia | Macedonia | Tajikistan |
| Comoros | Madagascar | Tanzania |
| Congo | Malawi | Thailand |
| Cook Islands | Malaysia | Togo |
| Costa Rica | Maldives | Tonga |
| Croatia | Mali | Trinidad and Tobago |
| Cuba | Malta | Tunisia |
| Cyprus | Mauritania | Turkey |
| Czech Republic | Mauritius | Turkmenistan |
| Côte d'Ivoire | Mexico | Uganda |
| Denmark | Moldova | Ukraine |
| Djibouti | Mongolia | United Arab Emirates |
| Dominican Republic | Montenegro | United Kingdom |
| Ecuador | Morocco | United States |
| Egypt | Mozambique | Uruguay |
| El Salvador | Myanmar | Uzbekistan |
| Equatorial Guinea | Namibia | Vanuatu |
| Eritrea | Netherlands | Venezuela |
| Estonia | New Zealand | Vietnam |
| Ethiopia | Nicaragua | Yemen |
| Fiji | Niger | Zambia |
| Finland | Nigeria | Zimbabwe |
| France | Norway | |
| French Polynesia | Oman | Total: 184 |

**Table A2:** Summary Statistics for Trade and Tariffs by Commodity

| Commodity | Variable | Observations | Mean | Std. Dev. | Max |
|---|---|---|---|---|---|
| Beef | Intranational trade | 6,552 | 477.9 | 2,295.5 | 37,656.0 |
| | International trade | 1,526,616 | 0.6 | 19.4 | 7,946.3 |
| | Tariff (%) | 1,106,189 | 25.6 | 37.0 | 341.2 |
| Chicken | Intranational trade | 6,552 | 469.2 | 1,966.5 | 42,342.4 |
| | International trade | 1,526,616 | 0.3 | 9.6 | 1,413.8 |
| | Tariff (%) | 1,106,189 | 22.1 | 30.9 | 398.1 |
| Maize | Intranational trade | 5,060 | 684.3 | 5,612.9 | 117,603.3 |
| | International trade | 1,158,740 | 0.5 | 19.3 | 5,129.4 |
| | Tariff (%) | 914,265 | 10.9 | 45.7 | 499.4 |
| Pork | Intranational trade | 6,552 | 678.8 | 6,108.6 | 170,611.4 |
| | International trade | 1,526,616 | 0.4 | 13.0 | 2,895.3 |
| | Tariff (%) | 1,096,830 | 22.8 | 34.9 | 418.4 |
| Rice | Intranational trade | 5,060 | 844.9 | 5,622.8 | 118,177.8 |
| | International trade | 1,158,740 | 0.4 | 9.2 | 2,231.4 |
| | Tariff (%) | 914,265 | 21.0 | 90.9 | 1,177.7 |
| Soybeans | Intranational trade | 5,060 | 219.5 | 1,666.2 | 32,704.7 |
| | International trade | 1,158,740 | 0.7 | 74.8 | 27,235.1 |
| | Tariff (%) | 914,265 | 7.6 | 35.9 | 508.6 |
| Wheat | Intranational trade | 5,060 | 452.3 | 2,543.8 | 55,064.3 |
| | International trade | 1,158,740 | 0.7 | 17.5 | 3,716.2 |
| | Tariff (%) | 914,040 | 8.8 | 22.9 | 223.8 |

*Notes:* Table reports summary statistics for intra- and international trade and tariff rates for the seven commodities in our sample. Inter- and intranational trade flows are reported in current millions of U.S. dollars, while tariffs are reported in percentage terms. The minimum observed value for each variable is equal to zero.